

# Interfacing Biology and Electronics with Memristive Materials

Ioulia Tzouvadaki, Paschalis Gkoupidenis,\* Stefano Vassanelli,\* Shiwei Wang, and Themis Prodromakis\*

Memristive technologies promise to have a large impact on modern electronics, particularly in the areas of reconfigurable computing and artificial intelligence (AI) hardware. Meanwhile, the evolution of memristive materials alongside the technological progress is opening application perspectives also in the biomedical field, particularly for implantable and lab-on-a-chip devices where advanced sensing technologies generate a large amount of data. Memristive devices are emerging as bioelectronic links merging biosensing with computation, acting as physical processors of analog signals or in the framework of advanced digital computing architectures. Recent developments in the processing of electrical neural signals, as well as on transduction and processing of chemical biomarkers of neural and endocrine functions, are reviewed. It is concluded with a critical perspective on the future applicability of memristive devices as pivotal building blocks in bio-AI fusion concepts and bionic schemes.

## 1. Introduction


Organs and systems in the human body rely on a combinatory scheme of electrical and chemical signals that ultimately offer a broad repertoire of potential biomarkers. While capturing those

diverse signals is the “hunting ground” of biosensing technologies, making use of them requires extracting and quantifying patterns that carry relevant functional information. As the repertoire of biosensors broadens along with their resolution,<sup>[1]</sup> the challenge mounts of processing the growing pool of streamed data, and these eventually in real time and with low power consumption for implementation in implantable or wearable biomedical devices and bioelectronic medicines (Figure 1a) and in lab-on-a-chip systems. The interest naturally goes toward devices with the potential of overcoming main bottlenecks such as, above all, the physical separation between sensing, processing, and actuating modalities that limits the form factor, latency, and energy

efficiency of current systems and that becomes more pronounced when large-scale, real-time, and long-term monitoring is required. In this context, novel memristive materials and nanodevices could play a central role, thanks to their intrinsic low power operation and their full compatibility with conventional complementary metal–oxide–semiconductor (CMOS) technologies for large array integration, coming into play for processing biosignals either in the form of all-or-none events or as complex spatiotemporal patterns.

Many biological signals come in the form of events by nature. Neuronal spikes represent a striking example relevant for applications such as the intraoperative positioning of deep brain stimulation electrodes in Parkinson's patients or for driving prostheses based on brain–machine interfaces (BMIs) (Figure 1b,c). Memristors are recognized as capable of emulating synaptic processing of spikes<sup>[2]</sup> and therefore appear as an ideal physical link between brain and electronics.<sup>[1]</sup> Recorded spikes typically require fundamental processing steps to extract quantitative information on neuronal activity: detection of the spike events, sorting (i.e., classification depending on features), counting over time windows are among the most used operations to characterize neuronal firing. As reported in Section 4 of this review, single memristors can, at least in part, take over these tasks. Alternatively, in the context of more complex and unconventional digital architectures, memristors can perform higher level operations such as patterns recognition and complex features extraction (e.g., in the view of application in BMI) to the benefit of artificial intelligence (AI) running on compact low-power consumption processors (Figure 1b–d). Thus, closed-loop schemes

I. Tzouvadaki  
Centre for Microsystems Technology  
Ghent University–IMEC  
Ghent 9052, Belgium  
P. Gkoupidenis  
Max Planck Institute for Polymer Research  
55128 Mainz, Germany  
E-mail: gkoupidenis@mpip-mainz.mpg.de  
S. Vassanelli  
NeuroChip Laboratory and Padova Neuroscience Centre  
University of Padova  
Padova 35129, Italy  
E-mail: stefano.vassanelli@unipd.it  
S. Wang, T. Prodromakis  
Centre for Electronics Frontiers  
The University of Edinburgh  
Edinburgh EH9 3JL, UK  
E-mail: t.prodromakis@ed.ac.uk

 The ORCID identification number(s) for the author(s) of this article can be found under <https://doi.org/10.1002/adma.202210035>

© 2023 The Authors. Advanced Materials published by Wiley-VCH GmbH. This is an open access article under the terms of the Creative Commons Attribution License, which permits use, distribution and reproduction in any medium, provided the original work is properly cited.

DOI: 10.1002/adma.202210035

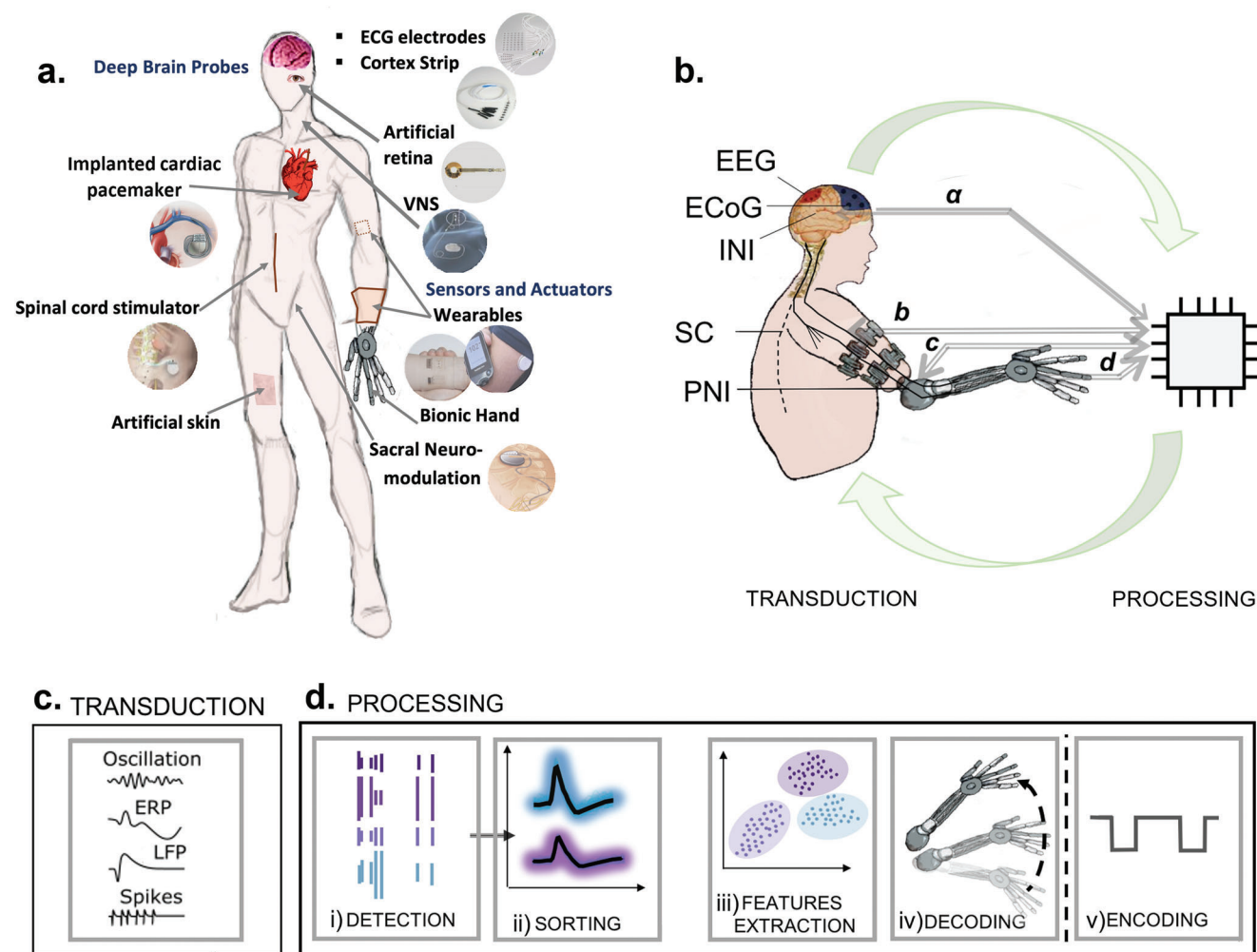


**Figure 1.** Essential building blocks and paradigms of BMIs and bioelectronic medicines. a) Highlights of the achievements in bioprostheses and bioelectronic medicines to probe, interface with, and assist the human body, i.e., wearable and implantable sensors and actuators, artificial parts, and implants. b) Illustration of a bidirectional brain computer interface paradigm comprising a close-loop context from nervous system and prosthesis to the artificial processing unit and vice versa. A general scheme comprises brain, spinal cord, or nerves as well as a robotic part, hereby a robotic arm. Recordings either from the brain or spinal cord (SC) ( $\alpha$ ), or from the nerves and prosthesis sensors (b, c, d) (forward cycle, i.e., transduction to processing) are processed, elaborated, and then provided as feedback (backward cycle) for stimulation of, e.g., nerves or muscles or to directly control movement of the artificial arm. The different modalities of signal transduction are indicated: Electroencephalography (EEG), electrocorticography (ECoG), implanted neural interfaces (INIs), SC, and peripheral nerve interfaces (PNIs). c) Transduction block indicating examples of signals described in detail in Figure 2 (oscillation and ERP for noninvasive, LFP and Spikes for invasive interfacing modalities). d) Processing block comprising a chain of distinct sub-blocks (i–v), i.e., detection–sorting–features extraction–decoding–encoding. Memristors can be part of the processing chain and, in perspective, merging transduction with processing acting as smart sensors.

with brain, peripheral nerves, and organs of the human body promise significant advances in neuroprosthetics and bioelectronic medicines.<sup>[1–3]</sup> As discussed in greater detail in Section 2, other brain electrical signals in addition to spikes and originated from populations of neurons represent promising biomarkers. They include oscillations and evoked wave responses such as event related potentials (ERPs) and local field potentials (LFPs) (Figure 2),<sup>[4]</sup> each posing specific processing challenges particularly in the context of a prolonged mapping and continuous data stream.

Chemical biosensors are further extending the signals repertoire of accessible biomarkers to neurotransmitters, or other biomolecules across the human body including hormones

and cytokines. It can be envisaged that they will be incorporated in wearables, minimally invasive and implantable devices, or tissue-like systems for in vitro drug discovery assays. However, while, e.g., an on/off analysis of blood or sweat sample can be already carried out rather efficiently with current sensing and actuating electronic systems, continuous monitoring and data processing remains a severe challenge.

In this review, we discuss on the potential of memristive technologies as efficient and dynamic bridge between engineering and biology, establishing a direct and functional communication between the two parts to extract information out of biological data. We conclude by expressing some views of where such

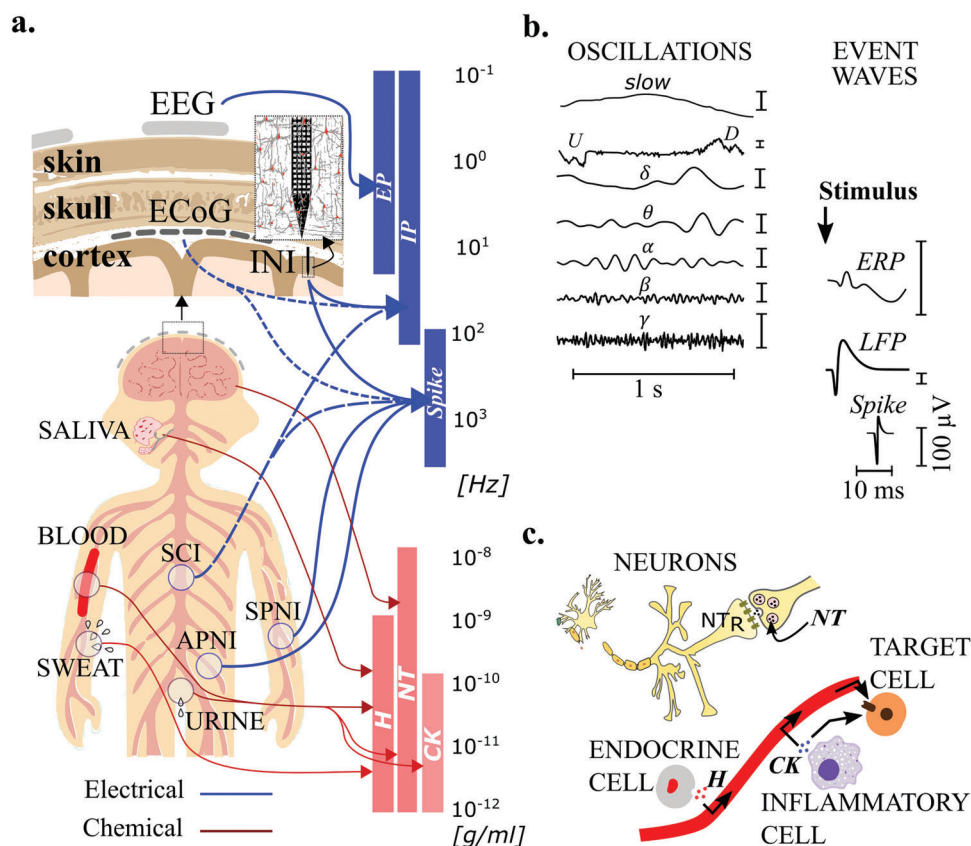


**Figure 2.** Electrical and chemical signals sensed throughout the human body. a) Brain electrical signals are measured extracranially by EEG, or intracranially by electrocorticography (ECoG) and implanted neural interfaces penetrating the brain tissue (INI). Specific neural interfaces can record from other structures of the nervous system such as the spinal cord (SCI) and peripheral nerves, either somatic (SPNI) or autonomous (APNI). Recorded signals depend on the measuring method and typically consist of changes of electrical potential: extracranial potential (EP), for EEG, and intracranial potential (IP), for invasive devices. ECoG and INI electrodes record the potentials generated at the surface of the brain cortex and inside the brain tissue, respectively. Both can measure field potentials generated by populations of neurons (i.e., local field potentials (LFPs)), and extracellular spikes from single neurons. Colored blue bars: approximate signal bandwidths (arrows connect the recording method to the signals covered). Body fluids contain chemical biomarkers such as neurotransmitters (NTs), hormones, and cytokines (CKs). Colored red bars and arrows indicate typical concentration ranges for each class of substances. b) Examples of brain signals approximately distributed depending on their dominant frequencies (frequency scale in (a)). Oscillations span from slow periodic waves and up/down states (U/D) to the gamma waves. Examples of stimulus-evoked event waves include spikes, LFP (both recorded intracranially), or event related potentials (ERP) measured by EEG. c) Schematic drawing of chemical biomarkers throughout the human body such as synaptic released NTs, hormones (H) secreted by endocrine cells, and cytokines (CKs) from inflammatory cells. Different biomarkers and biological sources are positioned according to typical concentrations (concentration scale in (a)).

technological advancements may potentially lead as applications in biomedicine.

## 2. An Overview of Biosignals

Electrical and chemical signals can be sensed throughout the human body and quantified becoming indicators of functional states, or biomarkers (Figure 2).

### 2.1. Electrical Biosignals

There are a variety of electrical signals originating from the nervous system.<sup>[5]</sup> Electrical signals are measured by electroencephalography (EEG), electrocorticography (ECoG), or implanted neural interfaces (INIs) penetrating the brain tissue typically

based on multielectrode arrays (MEAs). They can all convey a large amount of data. In the INI case, for example, a four probe arrangement with 32 microelectrodes each generates up to  $\approx 2$  Mbytes per probe  $s^{-1}$ . Advanced CMOS-based MEA probes comprising hundreds of recording sites reach a data rate of  $\approx 20$  Mbyte  $s^{-1}$ . Similarly, neural electrical activity can be recorded by spinal cord (SC) implants and peripheral nerve interfaces, either somatic (SPNIs) or autonomous (APNIs) (Figure 2a). Moreover, electrical signals can be sensed from heart and muscles by electrocardiography and electromyography (not shown). In conclusion, a large repertoire of electrical signals can be streamed in real time offering opportunities for valuable biomarkers in therapeutic applications, which poses, however, a big data challenge.

Processing strategies to extract information from electrical biosignals depend on whether they are in the form of single events or periodic waves. Several electrical signals are in the form of events. As already mentioned, spikes recorded by

implanted probes are all-or-none signals by nature (Figure 2b). Potential waves evoked in response to stimuli or motor actions and recorded extracranially by EEG (i.e., evoked response potentials or ERPs) are events too, along with evoked LFPs that are recorded intracranially (Figure 2b). Periodic signals, instead, comprise a large family including UP and DOWN states or sinewave-like oscillations that can be recorded by extra- and intracranial electrodes and are typically classified depending on the dominant frequency. Periodic signals range from below one, up to a few hundred Hertz (Figure 2b). They can last for long (e.g., minutes) and form complex signals (e.g., as nested waves) that require high-order processing. Noteworthy, all these signals (including spikes) are recorded extracellularly for clinical or lab-on-a-chip purposes, which implies that their amplitude is typically small (i.e., microvolts to few millivolts). Moreover, the fastest signals (i.e., spikes) are below a few kilohertz in bandwidth which, along with the small amplitude, rises challenges for memristor-based processing.

The bandwidth of the recording method has significant impact on measured signals. For EEG, because of skull attenuation and to avoid contamination from muscle activity, a standard upper frequency limit is set at around 30 Hz. Thus, the EEG spectrum typically spans from delta (0.5–4 Hz) up to beta (12.5–28 Hz) oscillations but can hardly reach the gamma range (about 30–150 Hz, varying across studies), and the same frequency spectrum limitation applies to ERP events. Invasive neural probes, that include ECoG grids placed in the epidural or subdural space above the brain cortex in addition to INI, expand the spatiotemporal resolution to cover the whole range of measurable brain activity, from oscillations and ERP to evoked LFP (<300 Hz) and spikes (<3 kHz) (Figure 2b).

## 2.2. Chemical Biosignals

Neurotransmitters (NTs) released by synapses, or hormones (H) and cytokines (CK) secreted by cells in body fluids can be sensed by chemical biosensors and represent potential biomarkers (Figure 2c). In neurons, in fact, an important form of chemical communication is expressed through spike-triggered NT release at the axon terminals and binding to the corresponding receptors of the target cell (either postsynaptic neuron, muscle cell, or gland cell).<sup>[6]</sup> In some cases, this form of communication can influence multiple neurons at once, e.g., through the diffusion of NTs out of the synaptic clefts (where concentration reaches the millimolar range). Nevertheless, NT concentration decays rapidly [ $t = 0.1$ – $1$  ms],<sup>[7]</sup> due to diffusion, reuptake, binding to receptors/transporters, or enzymatic breakdown). For example, among NTs, dopamine plays a crucial role in memory, attention, and learning functions.<sup>[8]</sup> It can act as an important biomarker (e.g., for diagnosis of neuroblastoma) and a normal concentration window (in serum or urine) is considered in the range from few to  $10 \text{ ng mL}^{-1}$ . Abnormal dopamine levels in the brain (excess or deficiency) may cause or be linked to several health conditions such as Parkinson's disease and other psychiatric disorders. Further to neurotransmitters, hormones (e.g., insulin, cortisol, thyroxine), and cytokines (e.g., tumor necrosis factor alpha, interleukin 6, and interferon gamma), are key markers of endocrine and immune functions, which are interrelated with those of the

nervous system.<sup>[9]</sup> Noteworthy, contrary to neurotransmitters in the synaptic space or its proximity, concentration changes of hormones and cytokines in blood and extracellular fluids tend to follow slow dynamics (typically from minutes to hours).

## 3. An Overview on Memristive Technologies and Materials

Memristors are devices whose internal resistance depends on the history of applied voltage and current. They provide to electronics a new dimension,<sup>[10]</sup> and may deliver highly scalable,<sup>[11]</sup> fast,<sup>[12]</sup> power-efficient (requiring minimum energy for operation capacity<sup>[13]</sup>), and reconfigurable electronic systems.<sup>[14]</sup> When compared to CMOS-based memory, memristors exhibit a multitude of states for less energy and space,<sup>[15]</sup> while their miniaturized size and simple, two-terminal architecture allow high integration density (e.g., via a cross-point array) enabling in parallel computing and processing of large volume of input signals.<sup>[11]</sup> Thus, while entering the era of big data, memristor-based designs may outperform conventional digital approaches for hardware implementation of compute-intensive systems such as neural network accelerators with better power and area efficiency by directly addressing the memory bottleneck.<sup>[16]</sup> Memristors, however, can also function as analog processors (i.e., outside the digital scheme), e.g., emulating synaptic computation. This offers attractive opportunities in the field of biosensors and their biomedical applications, in terms of unconventional brain-inspired computing strategies and to avoid power-hungry analog-to-digital conversion.

Memristive systems nowadays involve a variety of different materials and architectures.<sup>[17]</sup> The most widely known building blocks for fabricating memristive devices usually comprise a stack of oxide active layer(s) such as tantalum oxides, titanium oxides, hafnium oxides, sandwiched between two metal electrodes, like, for instance, gold or platinum (Pt) of nanometer thickness or semiconductor materials like heavily doped silicon and indium tin oxide, resulting to devices overall known as metal–oxide memristors. Meanwhile, memristive technologies involving chalcogenides,<sup>[18]</sup> perovskites,<sup>[19]</sup> silicon,<sup>[20]</sup> 2D materials,<sup>[21]</sup> and liquid-based materials have also been reported.<sup>[22]</sup> Memristive behavior can be also expressed in systems purely comprising organic materials,<sup>[23]</sup> such as polymers and fully or partially engineered of natural, biological compounds.<sup>[24]</sup> Memristive structures can be fabricated as vertical layers (vertical stack) of cross-point arrays (in stand-alone or crossbar arrangement),<sup>[11,25]</sup> as well as planar (lateral) architectures,<sup>[26]</sup> and in the form of nanoscale configurations,<sup>[27]</sup> such as nanowires,<sup>[28]</sup> and nanogaps.<sup>[29]</sup>

Additionally, memristive devices come in many “flavors” related to the underpinning switching mechanisms, and characteristics,<sup>[15a,30]</sup> such as thermal–chemical mechanism,<sup>[31]</sup> phase change,<sup>[32]</sup> electrochemical metallization, valence change memory.<sup>[33]</sup> The origin of switching,<sup>[30]</sup> and consequently the hysteresis appearing in the current to voltage characteristics of nanoscale devices exhibiting memristive characteristics, can be attributed to a wide range of phenomena including redox-based events, the drift of oxygen vacancies,<sup>[34]</sup> (e.g., in valence-change mechanism, the creation and electromigration of oxygen vacancies induce the distribution of the carrier density and



the valence states of cations,<sup>[35]</sup> and/or interstitials,<sup>[36]</sup> filament formation<sup>[37]</sup>). The formation process can occur either abruptly (binary) or gradually (analog), within an active core under the influence of an applied electric field (e.g., in fuse–antifuse mechanism, metallic filaments are created through the insulator matrix during the electroforming process and are fused as a result of Joule heating and the electric field). Furthermore, memory effects are also attributed to the finite mobility of ions as they redistribute within a charged nanopore under applied potentials and, more specifically, due to noninstantaneous ion redistribution. Thus, these effects are considered to originate from the dynamic properties of charge carrier ions.<sup>[38]</sup>

Irrespective of diversities in the underpinning physics, all memristive devices have in common a reconfigurable resistance that correlates to synaptic weights in biological neurons. Interestingly, resemblances, however, do exist as exemplified by metal/oxide resistive random-access memory technologies (ReRAM or RRAM)<sup>[30]</sup> (we adopt in this review a widely accepted notion that ReRAM/RRAM is a class of memristors<sup>[10,39]</sup>). ReRAM has two terminals, (top and bottom electrodes) that remind the pre- and postsynaptic neurons, and the switching layer in-between that recalls the synaptic cleft. At a closer look, however, a significant difference emerges. ReRAM can be programmed to a multitude of distinct resistive states,<sup>[15b]</sup> thus indeed reminding the tuning of the postsynaptic membrane conductance by NT and plasticity. However, ReRAM relies on the switching layer that is dynamically reconfigured when stimulated by electrical input causing physical ion migrations/redistribution associated to chemical redox processes within the film. Thus, the role of NTs and molecular signaling networks in the biological synapse is taken over by a much simpler physical mechanism in ReRAM: the direct electrical tuning of ion motion in the switching material.

Despite the physical diversity with respect to the biological counterparts, owing to their ability to emulate a variety of processing and storage functions of synapses in biological neural networks,<sup>[2]</sup> memristive technologies have been proven excellent candidates for neuromorphic,<sup>[40]</sup> brain-inspired computing<sup>[25,41]</sup> and artificial neural networks (ANNs),<sup>[40b,42]</sup> AI,<sup>[43]</sup> pattern classification<sup>[44]</sup> and learning.<sup>[45]</sup> These proved the memristor as a remarkable “more-than-Moore” device that emerged as a strong addition to the traditional technologies relying on CMOS scaling which has been slowing down, is facing challenges, and will meet headroom in the future.<sup>[46]</sup>

#### 4. Memristive Technologies for Biosignal Processing – Electrical Modality

A mounting challenge for neural interfaces and their application perspectives as implantable systems is how to process the increasing volume of sensor output data in real time and in a context of stringent constraints on power and size form. Processing in the “cloud” or external workstations does not represent a real solution as it requires high speed data links which, apart reliability and security challenges, rely on bulky and/or high-power wireless transmitters or wired cables.<sup>[47]</sup> Let us consider a practical example: state-of-the-art technologies offer hundreds to thousands of sensing nodes in a miniaturized front-end.<sup>[48]</sup> However, the algorithms to process the data cannot be run on an implantable

device yet.<sup>[49]</sup> Memristive technologies offer a new prospective solution to address this challenge, both in terms of analog processing strategies and in the context of hybrid analog/digital or digital architectures. For example, as reported below, physiological event signals such as spikes generated by neural activity can be efficiently detected, integrated, and even sorted via the analog thresholded nature of the memristive systems, thus avoiding digitization. The single memristor is driven by recorded spikes from neurons once duly amplified, undergoing switching events that can be used for spike detection and counting as well as for temporal integration like in biological synapses (**Figure 3a,e,f**). On a similar basis, the different analog responses of a memristor to different spike waveforms as recorded from the living neurons can be used for sorting (**Figure 3c,d**). In a more general framework, signals recorded by neural probes could be used as input to memristor arrays and artificial neural networks for extraction of parameters of interest, exploitable in future applications as biomarkers for diagnosis or for prosthetics (**Figure 3b**).

A simple, yet potentially very useful operation rule for processing recorded spikes as analog signals is the so-called memristive integrating sensor (MIS) platform.<sup>[50]</sup> A fundamental aspect of the working principle is that, after suitable preamplification of recorded spikes, they are applied without any digitization as input to the memristive system, which signifies the registration of an occurring event as a change in the corresponding state variable. Thus, in essence, the changes in the device state-variable levels are exploited to encode neuronal firing information by performing signal detection and integration of spiking activity, i.e., emulating temporal integration of biological synapses. The MIS was showcased utilizing raw biosignals originating from spiking activity of retinal ganglion cells recorded from a MEA front-end system, and preamplified through inbuilt amplifiers. Thus, signals are voltage–time series which are the input to the MIS platform and information on spike amplitude and frequency is transduced via a gradual (analog), saturating switching that encodes multiple spiking events via a single memristive element as nonvolatile resistive state transitions. Noteworthy, instead of digitizing the full voltage time series as it would be in case of conventional systems, in this case digitalization is only realized periodically for readout of stored spiking information from the memristor, ultimately retaining only a limited yet representative amount of data. Another, yet more complex analog processing strategy was adopted for spike sorting,<sup>[51]</sup> i.e., the recognition and then classification of spikes from different neurons based on the different shapes of their voltage waveforms. In this case, it has taken advantage from the fact that the dynamics of a memristor change represents the envelope of the input parent spike (**Figure 3a**).

Forward looking, low threshold memristors may allow complete independence from signal-amplitude amplification requirements and additional intermediate agents. The direct transduction of electrical signals from neurons without preamplification or intermediating agents, but entirely through a two-terminal organic memristive device signifies an important step to this direction.<sup>[52]</sup> The scheme is implemented for unidirectional, activity-dependent coupling of two live neurons in brain slices. In this case, the neuronal activity was recorded intracellularly, and the excitation threshold in the postsynaptic neuron controlled the values of the device resistance. Additionally, protein-nanowire-based memristors are reported and schemes able to function at

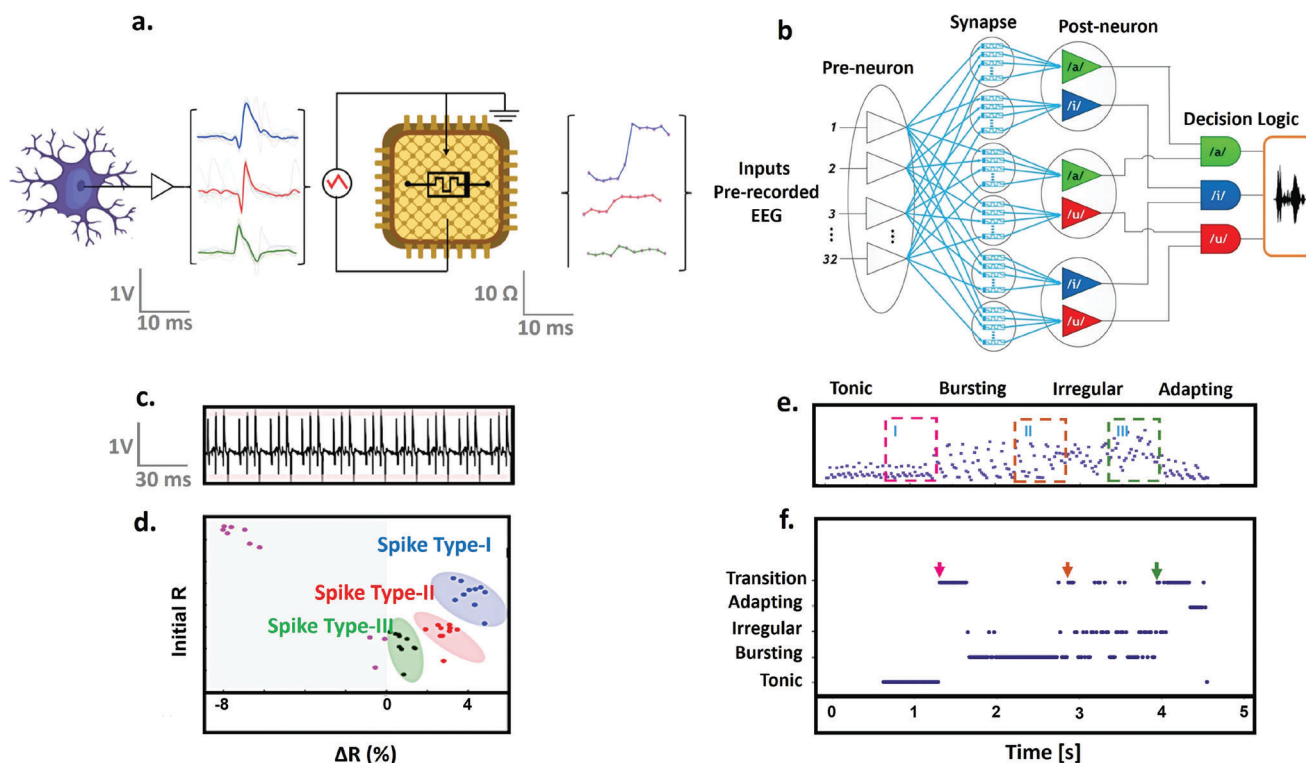


**Figure 3.** Memristors for neural signal processing and information processing. a) Concept illustration where spikes suitably amplified are used as input to the memristive spike sorter, which links different types of spikes of various strengths and shapes, generated by different neurons and, consequently, featuring different signature waveforms. The response of memristive devices is a change in resistance corresponding to the envelope of the single spiking event. b) Binarized features extracted after the processing of collected EEG signals (vowel features from speech imagination) are used by a memristive preneuron's block. A leaky integrate-and-fire neuron is used in the postneuron block, where the postneurons are paired into groups comparing vowel duets. Decision logic determines which postneuron fires first based on their output signals. c) Succession of different spike waveforms. d) Such spike waveforms utilized as input for the spike classification, overall identifying three different clusters with respect to spike type, through the change in resistive state versus starting resistive state for each pair of consecutive measurements taken. e) Indicative experimentally measured memristor response to a streaming spike train with clear correlations to the firing patterns and transitions (I "Tonic → Bursting," II "Bursting → Irregular," and III "Irregular → Adapting"). f) Obtained outputs from the network over time, highlighting the detected pattern transitions. (a), (c), (d) Reproduced with permission.<sup>[50]</sup> Copyright 2016, Nature Publishing Group. (b) Reproduced with permission.<sup>[45a]</sup> Copyright 2015, Nature Publishing Group. (e), (f) Reproduced with permission.<sup>[54]</sup> Copyright 2022, Nature Publishing Group.

very low power and same voltage levels as the brain, namely in the range of biological action potentials.<sup>[23,53]</sup>

While classification of signals in this instance is happening using the thresholded integration capability of memristors, more conventional neuromorphic types of classifiers can be implemented. Employing memristive architectures provides an energy-efficient and reconfigurable strategy for large-scale computing applications.<sup>[14]</sup> A memristor-based reservoir computing system has been reported,<sup>[54]</sup> where the memristor was directly driven by emulated neural spikes, firing patterns and transitions (Figure 3c), while its state reflected temporal features of the spike train (Figure 3f). A memristor-based neural network has been also implemented in classification of EEG-represented brain states for learning and recognizing imagined speech patterns corresponding to speaking vowels.<sup>[45a]</sup> The system operation was based on capturing and processing vowel-related EEG signals, extracting the distinct features and converting them to binarized input to a memristive hardware neural network (HNN). The applied to the memristive HNN feature codes, were ultimately recognized by an integrate-and-fire postneuron scheme,

combined with decision logics determining which postneuron fires first based on the output signals (Figure 3b). Additionally, a spiking neural network compatible for implementation in a neuromorphic device is applied for the detection of high frequency oscillations generated by epileptogenic tissue.<sup>[55]</sup>

Meanwhile, current trends in the BMI era are reported by Neuralink with the interest going toward scalable, high-bandwidth, flexible, and fully implantable BMI systems, showcasing a prototype comprising ultrafine polymer probes and miniaturized custom high-density electronics that allow streaming of full broadband electrophysiology data simultaneously from all the electrodes under consideration.<sup>[56]</sup> Besides, hardware design combined with analysis of signal quality and decoder performance of neural signals collected from experimental intracortical BMIs (iBMIs), opens new opportunities for the development of wireless iBMIs that are considerably power efficient without loss of performance.<sup>[57]</sup> Memristor arrays were also utilized in the concept of a BMI scheme, to implement filtering and identification of epilepsy-related brain states, via integration with neural interfaces.<sup>[58]</sup> The memristors are implemented both as signal

preprocessors (Finite Impulse Response or FIR filter bank) and as decoding elements (classification or regression task) overall comprising one array-based neural signal analysis system. The core of the system is the memristor array translating the neural signals (LFP signals recorded in real-world setting) into control commands for the external effectors. Considering that the brain dynamics and the neural signals are related in several specific frequency bands, the frequency-related information may allow the distinction between the different brain states. Thus, information from filtered signals concerning waveform amplitude and energy at each frequency band is extracted and fed to a single-layer perceptron neural network to identify the epilepsy-related brain state that is characterized as normal (no epileptic neural activity), interictal (epilepsy between seizure events), and ictal (epileptic seizure event in the brain). Additionally, an effort toward epilepsy prediction has been demonstrated through a multichannel neural signal processing system based on one transistor–one resistor memristor arrays.<sup>[59]</sup> In this system, the energy and variation information of the input neural signals are extracted by leveraging the inherent memristor conductance modulation, where the critical information of neural signal waveform is ultimately extracted and encoded. The system is validated through the processing of a 16-channel iEEG signals demonstrating high-accuracy seizure prediction with more than 95% accuracy; the power consumption in each channel is estimated to be only 60.81 nW per channel, which indicates an energy efficiency that has not been achieved with any conventional technologies.<sup>[60]</sup> A detailed comparison between memristor-based and conventional designs is available in Section S3 of the Supporting Information.

Further applications involving memristive/neuromorphic technologies in monitoring and processing of biomedical electrical signals include embedded systems able to process electromyography (EMG) signals locally on the electrodes side (e.g., performing EMG classification using reservoir computing, following the conversion of the EMG signal to spikes),<sup>[61]</sup> as well as implemented for classification of physiological/abnormal activity of cardiac intervals.<sup>[62]</sup> For instance, a neuromorphic computing system consisting of a two-layer architecture of crossbar array is applied for a real-time cardiac arrhythmia monitoring through classification of different beat types.<sup>[62]</sup> The first crossbar layer corresponded to the synaptic weights connecting the input and hidden neurons. Raw electrocardiogram data are directly used as input, normalized, and mapped. Following the signals' collections from crossbar first layer, they are applied in a similar way to the second crossbar layer. Finally, the output signals representing the possible beat types are applied to the decision-making block giving a system prediction of the corresponding class.

## 5. Memristive Technologies as Biotransducing Elements – Chemical Modality

Electrochemical (bio)sensing schemes of memristive nature and properties have recently drawn particular attention (Figure 4).

For example, electrochemical memristors can be activated via bio-electrocatalytic glucose oxidation and integrated with a biomolecular computing system and operating in combination with enzyme-based logic systems (Figure 4a).<sup>[63]</sup> Such systems

comprise a biocatalytic cascade mimicking the operation of concatenated logic gates and the control is imposed by the logically processed inputs of glucose and oxygen. In addition, electrochemical systems with memimpedance and memcapacitance properties (that depend on the state and history of the system and are caused by combinations of nonlinear electric responses) are also showcased.<sup>[64]</sup> The scheme depicts transitions between open/closed states originated from the bulk electrolysis of hydrogen peroxide that results in solution pH changes. Chemical signals such as neurotransmitters release into the synapse, govern connectivity between neurons. To realistically emulate the function of biological synapses, the synaptic weight expressed by the neuromorphic device must be regulated in a dynamic way by a local neurotransmitter. The direct coupling of a neuromorphic device with dopaminergic cells was demonstrated,<sup>[65]</sup> achieving synaptic-like conditioning based on neurotransmitter-mediated signaling mimicking the natural dopamine action. Dopamine exocytosed by PC-12 cells at the presynaptic end, locally oxidized at the postsynaptic gate electrode, emulates the postsynaptic receptor binding observed in biological synapses changing the charge state of the gate electrode. This mechanism emulates the synaptic weight modulation by the neurotransmitter resulting to ion flow in the aqueous electrolyte, altering the conductance of the postsynaptic channel (Figure 4b). The PC-12 cells are stimulated with potassium chloride solution to elicit exocytosis and to monitor the dopamine release rate that elicits the postsynaptic voltage pulses and consequently controls the conductance modulation.

Besides, memristive technologies demonstrate a remarkable performance among electrochemical biosensors. Chemical and biological species such as proteins are composed of charged residues, hence demonstrating a net positive or negative charge. Consequently, the additional surface charges due to the biomolecules introduced in the system result in an increase/decrease in the overall net charge, modifying the effective local potential. When surrounding the memristive device (e.g., in the case of planar structures) (Figure 4c–f), these surface charges introduced act by creating an equivalent, virtual all-around biogate effect (Figure 4e–f), that is equivalent with the one depicted in the case of nanostructures without any biofunctionalization but fabricated with an all-around silicon gate (Figure 4c,d). Therefore, the net charge from the presence of biomolecules induces a change in the initial hysteresis creating a sort of voltage memory, defining a concentration and kind-dependent voltage difference between the current minima for backward and forward regimes that is related to capacitive effects and diffusion currents occurring in the system.<sup>[66]</sup> In the metal/oxide vertically stack memristor architecture, the charged organic molecules modify the effective local potential, ultimately acting equivalently to an electrical stimulus that imposes a shift in the device's memory state (Figure 4g–i). While a memristor reacts with a change in the state variable when subjected to an input stimulation (i.e., voltage pulse) of an amplitude that exceeds certain thresholds (Figure g,j), the state variable of a chemical memristor changes as a result of a chemical input (i.e., charges carried-on by the organic molecules or disease biomarkers) (Figure h,i), where the analyte has the role of the excitation parameter, ultimately leading to a label-free biodetection method.

The memristors are converted to target-specific sensing elements through surface biofunctionalization with target-specific

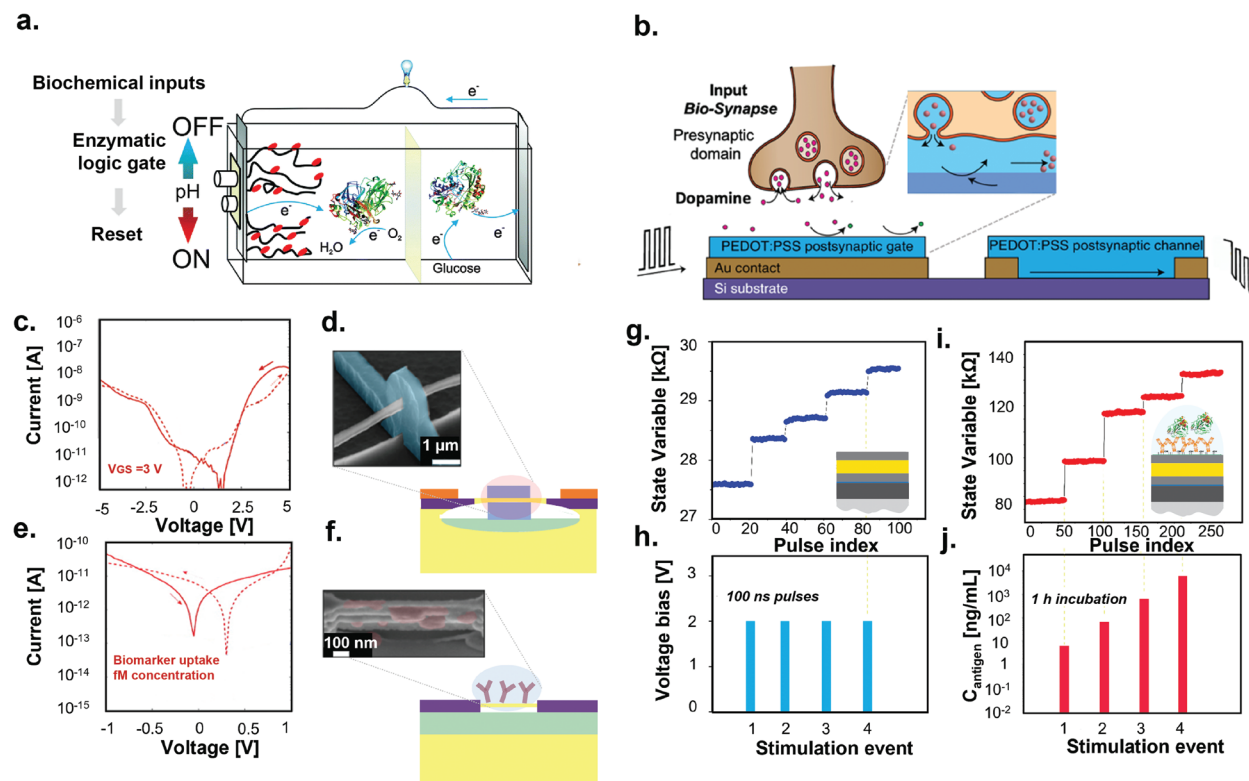


**Figure 4.** Memristors as biosensing elements. a) A switchable biofuel cell controlled by logically processed biochemical signals comprising pH-switchable bio-electrocatalytic electrodes and pH-change-producing enzyme logic system. The enzyme-induced pH changes ultimately switch the activity of the bio-electrocatalytic oxygen reduction at the modified cathode, between the ON and OFF states. b) Schematic illustration depicting artificial and biological neuron integration. The firing rate of the presynaptic neuron defines the dopamine concentration at the device–cell interface while the pulse rates of both the presynaptic and postsynaptic domains define the change in postsynaptic current (or long-term potentiation) ultimately resulting in a correlated spiking learning mechanism. c) Current-to-voltage characteristics ( $I_{DS}$ – $V_{DS}$ ) of gate-all-around nanowire FETs for a fixed back gate voltage ( $V_{GS}$ ). d) Gate-all-around silicon nanowire FET schematic illustrating the device concept. Polysilicon is deposited and patterned to form the gate. Metallic source and drain contacts ultimately form source-to-body and drain-to-body Schottky junctions. Chromium/nickel bilayers are patterned on top of the silicon pillars, partially covering nanowires at the anchor points, leading to the silicidation of the nanowire channel from the chromium/nickel bilayer toward the gated region of the nanowire. The scanning electron microscope image depicts the silicon nanowire surrounded by the gate. e) Current-to-voltage characteristics ( $I_{DS}$ – $V_{DS}$ ) of a freestanding Schottky-barrier silicon nanowire device functionalized with biological molecules. A voltage difference is introduced between the current minima in the current to voltage characteristics upon the presence of charged biological substances. The biological substances surrounding a freestanding silicon nanowire array that create a virtual all-around biogate acting in a similar way with the inorganic all-around-gate. f) Schematic illustrating a device of two-terminal freestanding Schottky-barrier silicon nanowire anchored between nickel-silicide terminals and biofunctionalized with biological molecules. The scanning electron microscope image shows the nanowire device and the covered by biological molecules. g) Transient response of a memristor's (stack of metal–oxide architecture) state variable in response h) to voltage input pulses. i) Transient response of a chemical memristor state variable in response to biochemical inputs rendering j) distinct antigen levels. While in the case of memristor a specific state can be achieved by modulating different voltage pulse characteristics, in the chemical memristor distinct concentrations of antigen are transduced via analogous memory-state changes by introducing a chemical state variable. (a) Reproduced with permission.<sup>[63]</sup> Copyright 2013, Royal Society of Chemistry (b) Reproduced with permission.<sup>[65]</sup> Copyright 2020, Nature Publishing Group (c–f) Reproduced with permission.<sup>[66]</sup> Copyright 2021, IEEE Sensors Council (g–i) Reproduced with permission.<sup>[73]</sup> Copyright 2020, Nature Publishing Group.

receptor molecules like, for example, antibodies or DNA aptamers. First, the device surface is treated with  $O_2$  plasma or Piranha solution for clearing organic residues and for generation free surface hydroxyl-terminating groups. Hydroxyl groups serve as surface treatment, enabling a stable chemical attachment of the biomolecules. Surface functionalization strategies such as direct absorption (physisorption), covalent binding, e.g., through the implementation of a silane and affinity methods (e.g., high affinity between biotin and streptavidin) for optimum coupling of the receptor molecules on the devices' surface. Following the biofunctionalization process, the sensors are implemented for biomarker sensing by exposure of the devices to the target solu-

tion. Morphological atomic force microscopy (AFM) analysis of two different memristor structures (a planar memristor consisting of a freestanding silicon nanowire and Schottky barriers and a vertically stack metal/oxide memristor architecture) is shown in **Figure 5** carried out on bare devices (Figure 5a,b) and after the biofunctionalization of the same devices with antibodies specific to prostate specific antigen (PSA) (one of the main biomarkers for Prostate Cancer) using the direct absorption functionalization strategy (Figure 5c,d) qualitatively revealing the presence of the biological substances on the surface of the memristors, that ultimately results in an increase of the surface features recorded as well as in the formation of some agglomerating patterns, due to



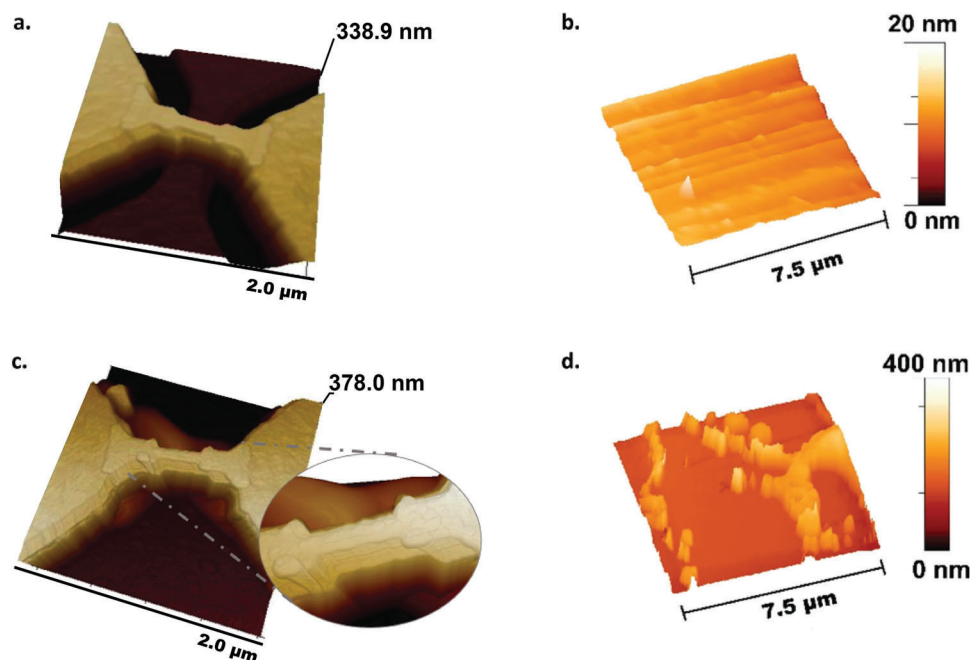


**Figure 5.** Memristors surface morphology before and after surface biofunctionalization with an anti-prostate-specific-antigen antibody, obtained with atomic force microscopy (AFM). a) AFM morphological analysis of silicon nanowire structures before biofunctionalization. b) Metal/oxide memristor's Pt top-electrode surface before functionalization. c) Silicon nanowire structures after the biofunctionalization with  $250 \mu\text{g mL}^{-1}$  anti-PSA antibodies and d) the Pt top-electrode surface of the metal/oxide memristor after the biofunctionalization with  $200 \mu\text{g mL}^{-1}$  anti-PSA antibodies. Reproduced with permission.<sup>[66]</sup> Copyright 2021, IEEE Sensors Council.

coalesced biological molecules, that are depicted in the form of high peak wrinkles. Especially for the bare nanowire device (Figure 5a), the shape of the nanowire is clearly distinct. After biofunctionalization, a clear change in the morphology can be seen in Figure 5c and agglomeration of biomolecules can be observed on the devices' surface.

Memristive biosensors present a versatile approach for antigen-specific transduction,<sup>[67]</sup> as the sensors' specificity can be determined in an ad hoc manner via biofunctionalization and achieved ultrasensitive sensing capabilities (limit-of-detection in attomolar range) showcased for PSA.<sup>[67]</sup> Other applications involve glucose,<sup>[68]</sup> acetylcholine,<sup>[69]</sup> granzymes and interferon-gamma,<sup>[70]</sup> brain cancer,<sup>[71]</sup> Ebola matrix protein,<sup>[72]</sup> and for the detection of immune attack in sections of breast cancer patient tumor biopsy.<sup>[73]</sup> The inherent state programmability and reconfigurability attributes of the memristors,<sup>[14]</sup> offer the additional benefit of the in situ, at-device-level calibration of entire biosensing arrays,<sup>[73,74]</sup> resulting in a homogeneous sensing baseline across the individual cells, addressing the longstanding bottleneck of generated offsets and variable responses across the sensing cells, and can be readily used for sensing without resorting to external software/hardware calibration approaches. The properties of ultrasensitivity and inherent state programmability and reconfigurability expressed by the memristor-based sensors render them a valuable alternative technology to the conventional CMOS-technology-based biosensor systems and, for instance, in this framework, the biosensor field-effect transistors (BioFETs).<sup>[75]</sup> Moreover, in cases where particularly high sensitivity is required and/or large biosensing panels are involved, where the intersensor variation can mask the biosensing outcome and

the at a common sensing baseline is essential for a reliable sensing, memristor-based biosensors can be considered as a more advanced solution and suitable solution comparing to the conventional technologies. Additionally, thanks to their scalability,<sup>[11]</sup> properties enabling high array densities, and their integration compatibility with fluidics,<sup>[74]</sup> in perspective, such technologies can be challenged and utilized in more complex sensing schemes as, for example, large-area, multipanel diagnostic capabilities for the development of diagnostic tools allowing large throughput of tested specimen and facilitating the detection of multiple analytes per patient.

## 6. Perspectives

Memristive technologies have been employed to support challenging new systems and applications. In particular, following the memristor's physical implementation that was suggested in 2008,<sup>[76]</sup> the research interest in memristor technologies is constantly growing and, apart from many technical publications, resulted in a plethora of patents as well. More specifically, the number of international patent applications within a decade, depicted a significant rise (i.e., from 40 in 2005 to 158 in 2015).<sup>[77]</sup> Moreover, according to the Global Memristors Market – Growth, Trends, and Forecast (2019–2024), the memristor market was valued at USD 278.05 million in 2018. Looking in the present and forward, the International Market Analysis Research and Consulting (IMARC) Group now expects the memristor market size to reach a value of USD 1.7 billion by 2027. Regarding the memristor market segment analysis, and in particular, the industry vertical (or end-user industry), the consumer electronics as well

**Table 1.** Materials and concepts for memristive biointerfacing: electrical and chemical concepts for biointerfacing from (bio)signal transduction to the emergence of high-level functions to perceive and control biology.

	Electrical	Chemical
Monitoring	On-chip (bio)signal compression, <sup>[50]</sup> spike sorting thresholding <sup>[51a]</sup>	Dopamine detection, <sup>[100]</sup> sensing of cancer biomarkers, <sup>[67,73]</sup> organic artificial neurons for neuromorphic sensing/biointerfacing <sup>[78a,c]</sup>
Emulating	Memristor-built neurons, <sup>[23]</sup> neuronal coupling, 2D-memristor-based artificial synapses <sup>[101]</sup>	Biohybrid synaptic connection, <sup>[65]</sup> neuronal coupling/synchrony, <sup>[52]</sup> biorealistic organic artificial neurons <sup>[78a,c]</sup>
AI hardware	ECOG processing and classification, <sup>[59]</sup> epilepsy detection <sup>[58]</sup>	Time-domain classification in aqueous media, <sup>[102]</sup> in vitro closed-loop cell control <sup>[103]</sup>

as the information and technology and telecommunication sectors are expected to hold the highest market share, with an increasing demand for memristor devices that can deliver high-speed performance, due to the growing demand for high processing power and memory density, while maintaining the cost. This trend is highly driven by wearable and connected devices (USD 392.4 billion by 2030 according to Precedence Research). Healthcare, being one of the main pillars of the end-user industry will also note a significant growth, that is also highly related to the increasing trend in wearable technologies for monitoring physiological information for health and performance. Based on the applications, the neuromorphic and biological system segment is expected to own a key market share due to the introduced advancements in cognitive psychology and AI modeling. Considering that IMARC Group expects the neuromorphic chip market size to reach USD 8.6 billion by 2028, and the trends such as Neural Architecture Search, memristors can be a key technology for enabling the industry to realize the potential of such technologies. The combined properties and attributes of memristive/neuromorphic systems render these technologies capable for undertaking the sophisticated interfacing of electronics with biological systems, enabling real-time sensory processing, online classification and low-latency decision making, and ultimately power-efficient manipulation of physiological data of both electrical and chemical nature. **Table 1** summarizes representative concepts for interfacing biology with memristive technologies: from low-level biosignal transduction, and intermediate processing circuitry, to high-level emerging functions such as hardware. Electrical and bio/chemical concepts of signal manipulation are also indicated in this low-to-high level flow. While this review focuses on the most mature technologies, further opportunities may emerge involving memristive devices of different architectures and materials, unconventional form factors, and even more terminals, demonstrating different *modus operandi*.

Realizing and operating memristive technologies in close physical or functional proximity with biology, especially when dealing with long-term interfacing, involves a range of challenges. Current challenges include the realistic emulation of biological functionalities while ensuring biocompatibility and minimal side effects when in contact with biological tissues, as well as the prevention of potential mismatch between signal transduction and processing circuitries. Mismatch mitigation or even physical colocation in a single device entity of information processing and sensing modalities allows for efficient and compact concepts of biointerfacing. For instance, a memristive device that

performs computation (e.g., signal integration) while being sensitive to a host biological environment, can adjust its properties in situ, without needing separate sensing and computation units or signal transfer between them. A typical biorelevant environment is an aqueous electrolyte with alkaline ions (in physiological concentrations at the millimolar range), neurotransmitters, and neuromodulators (such as dopamine, glutamate, etc.). Recently, biorealistic organic artificial spiking neurons have been demonstrated in liquid operation and responsivity to common biomolecular species of the biological milieu.<sup>[78]</sup> Colocation of processing and sensing modalities is also necessary when chemical precursors are more prominent/occur earlier than electrical in the detection of biological phenomena of interest. Biomimetic approaches and emulation of biological functions/computational primitives can lead to advanced bioparameter matched computing systems facilitating a direct communication between electronics and biological processes. However, the functional similarity to biological systems without parameter matching and relevant metrics close to the biological regime (i.e., the metabolic efficiency of biological neurons and synapses), still requires additional circuitry for interfacing, adding costs to the vision of a seamless integration. For instance, energy-efficient and real-time biointerfacing requires device metrics such as operation voltages and response/relaxation time scales, that are close to those of biological events along with ultralow switching voltages and energy requirements (in the range of  $\approx 50$  mV,  $\approx 10$  pJ per event<sup>[79]</sup>). Although emulators of biological neurons exist, their operation voltages (approximately volts) are typically well above the amplitude of extracellular/intracellular action potentials (microvolt to millivolt).<sup>[40b]</sup> Protein-built memristors in the role of artificial synapses may function close to the biological regime.<sup>[23]</sup> Nevertheless, entirely biobuilt devices still have a performance gap comparing to their inorganic counterparts (i.e., endurance, stability, operation speed, and power consumption),<sup>[80]</sup> internal structure change under different working conditions, and limitations for forming designed micro/nanostructured patterns, e.g., with conventional lithographic techniques. Indicatively, the fundamental limit of a technology to be downscaled in dimensions, defines the ultimate potential of the technology in integration density and operational capacity. Toward this direction, memristor technology downscales aggressively in terms of dimensions and integration density (2 nm minimum critical dimension).<sup>[11]</sup>

On the other hand, monitoring in a continuous way, and in vivo directly from the human body increasingly shifts the research interest toward wearable or implantable devices.

Memristors can be involved in the realization of such schemes, undertaking the role of intelligent biointerfaces, dynamically transducing the chemical/biological signals via their inherent dynamic response. Taking into consideration that memristors function as thresholded integrators increasing the available time for measurements, namely when increasing the integration aspect,<sup>[50]</sup> the resulted confidence level will be significantly higher. Thus, even for the case of acquisition of noisy signals, if those signals are integrated long enough, valuable measurements can be successfully achieved. Thanks to their energy efficiency,<sup>[81]</sup> memristive technologies may overcome pivotal limitations reported in the wearables/implantable electronics field concerning high-power consumption. Adaptability and biocompatibility are essential properties for maximizing the acceptance rate of the device in a biological host. Memristive systems and ionoelectronic devices that consist of soft and/or organic materials,<sup>[22,24,78a]</sup> allow the artificial counterpart to follow or force the evolution of the biocircuitry over time, under natural or on-demand conditions, respectively, and are friendly to the biological environment.

However, the direct interfacing of biological tissues requires that the two domains are characterized by similar mechanical properties. Devices that consist of organic (semi)conductors are friendly to the biological host.<sup>[82]</sup> Electronic circuits of similar mechanical properties with biological tissues (approximately megapascal to kilopascal)<sup>[83]</sup> and substances (cells, tissues) enable conformal, (micro)motion/shape artifact-free biointerfacing, for long-term symbiosis of biology with electronics, minimizing the mismatch between neuromorphic electronics and biology.<sup>[84]</sup> Due to their soft nature, organic materials exhibit mechanical properties that are on the same range with biological substances (e.g., dura mater, skin, spinal cord, and brain). Direct biointerfacing exposes the electronics into a harsh, corrosive, and complex environment that contains water and various ionic and molecular species. Therefore, reliable biointerfacing requires robust materials, free of parasitic and side reactions with oxygen, ions, and water, especially when integrated in devices and systems for long-term recordings and stimulation. Indicatively, conducting polymers based on poly(3,4-ethylenedioxythiophene):poly(styrenesulfonate)(PEDOT:PSS) exhibit stable operation for  $\approx 4$  months when incorporated in microelectrode arrays for recording,<sup>[85]</sup> while being able to deliver a few billions of stimulation pulses.<sup>[86]</sup> Ideally, devices and systems for chronic biointerfacing require even further improvements in material reliability and endurance, while in-depth knowledge of the failure mechanisms is necessary for expanding the state-of-the-art boundaries.<sup>[87]</sup> Nevertheless, in controllable and non-biological environment, organic artificial synapses and nonvolatile memories are stable over a billion of write/erase cycles.<sup>[88]</sup>

Hardware/algorithmic codesign permits mutual technological hardware/software development on targeted ANN applications and mitigates hardware and device nonidealities (i.e., stochasticity/drift in switching voltages) via algorithmic design,<sup>[39d]</sup> while neuromorphic systems can complement conventional processors and high-performance,<sup>[89]</sup> 3D-integrated memristor can improve the system's ability to process large amounts of information – a critical need when dealing with big data.<sup>[10]</sup>

Apart from qualitative improvements and development (e.g., in reliability, endurance, integration, downscale of operation voltages), the introduction of new directions and material-related qualities, is necessary in memristive technologies for fulfilling the vision of seamless biointerfacing.<sup>[90]</sup> Efficient communication between electronics and biology requires even more of in materio computing, with computation and processing (i.e., conditioning, classification, multiplexing) that takes place locally due to intrinsic materials properties (e.g., via complexity, distributed physical properties, stochasticity, spatiotemporal phenomena, topological entities) and eases the computational load from supportive electronics. Bidirectional communication is also seamlessly enabled when both domains, electronics and biology, share the same computational primitives. This requires multimodality; for instance, synaptic plasticity and neuronal functions are not only emulated electrically but also biochemically, by considering the actual biological carriers of information (i.e., local/global electrolytes, alkaline ionic species, neurotransmitters, biomolecules, etc.). Such venture requires new approaches for in materio, iono-biochemical processing and recognition that is hard to be implemented only by capacitive/faradaic coupling of biology with electronics. In this way, computation, communication, and recognition will be tightly embedded on the edge, and at the actual interface.

**Figure 6** presents a comparison between the conventional biosensing and processing system and an envisaged memristor-based counterpart. From the sensing perspective, it adds electrochemical sensing capabilities to the conventional sensing modalities. Besides, one bottleneck of the conventional bio sensing systems is the requirement for relatively high-resolution and high-speed analog-to-digital converters (ADCs) to digitize the sensed biosignals and interface with the conventional digital signal processors. The abilities of memristors to process analog signals directly make it possible to address this bottleneck through system-level optimization.

As shown in Figure 6, in a memristor-based system, the ADCs are only needed to digitize processed results which require significantly lower resolution and speed compared to digitizing the raw signals at the sensing node. From processing perspective, the application of memristors in energy-efficient FIR filter banks, in-memory computing, and high-density, high-speed, and low-power nonvolatile memories benefit biosignal processing directly (Figure 6 Option 1). Besides, the high-density, low-power, high-speed access, and nonvolatile memory properties of memristors significantly reduces the energy consumption required in data movements. A detailed comparison between memristor-based and conventional designs for these core biosignal processing components is available in Tables S1–S4 (Supporting Information). Additionally, there are other alternative biosignal processing methods enabled by memristors. The MIS concept,<sup>[50]</sup> and memristive physical reservoir computing,<sup>[54]</sup> are emerging approaches for real-time large-scale neural signal analysis based on the premise that more efficient processing can be achieved by using the physical properties of memristors to process and compress the signals in situ and thus minimizing the latency and energy consumption induced in digitization, transmission, storage, and accessing of the massive amount of raw sensing data (Figure 6 Option 2). Besides, a truly bioinspired approach for biotransduction and processing can be facilitated by memristors

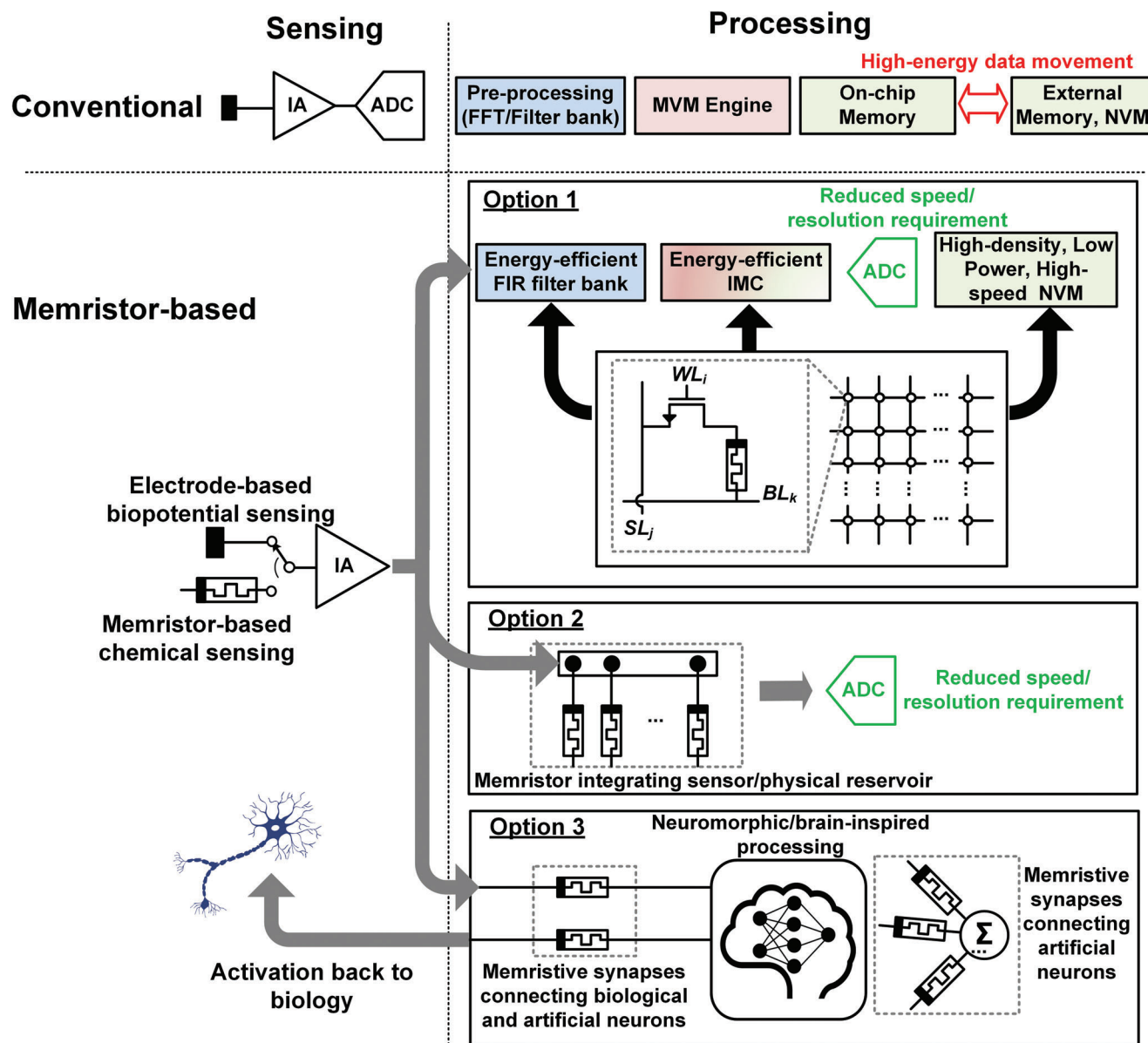


**Figure 6.** Comparison between the conventional and memristor-based biosensing and processing systems. The fundamental circuit components in conventional biosensing systems are instrumentation amplifiers (IAs) and analog-to-digital converters (ADCs) which amplify and digitize the sensed signals. The main components in the processing system include preprocessing unit which typically runs time–frequency analysis such as fast Fourier transform (FFT) and filter bank processing, matrix–vector multiplication (MVM) engines which are the core units to accelerate typical biosignal classification algorithms, and memory units including both volatile and nonvolatile RAMs. The CMOS technology allows integration of almost all the circuit components on a single chip, except that external memories are typically required due to the limited on-chip memory capacity. Memristor as a sensing element brings electrochemical sensing capabilities in addition to the conventional biosensing modalities. The sensed signals do not need to be digitized for further processing because of memristor-based processing interface with analog signals directly, eliminating the power consumed by a high-resolution, high-speed ADC at the sensing node. There are multiple approaches for memristor-based processing. First, memristor crossbars can be used to facilitate the chip implementation of the individual components in the conventional biosignal processing architecture, leading to more energy efficient FIR filters, in-memory MVM computing, and higher on-chip memory capacity to reduce the energy overhead required for accessing external memories (Option 1). The advantages of the memristors in these aspects are presented in Tables S1–S4 (Supporting Information). Second, nonconventional biosignal processing methods have emerged to use memristors to process the biosignals directly, utilizing the device state-variable levels to detect and integrate neuronal firing activities (MIS) or to implement physical reservoir computing that are efficient to process temporal inputs such as biosignals (Option 2). Note that in both Option 1 and Option 2, the ADC is only needed to digitize the processed results which require significantly reduced speed and resolution compared to digitizing the raw signals at the sensing node. Third, analysis of biosignals with neuromorphic or brain-inspired processors can be facilitated by memristors; they can be used to implement artificial synapses connecting artificial neurons leading to more efficient neuromorphic processors, and also to interconnect the artificial neurons with the biology creating opportunities to enhance the performance of brain-inspired processors by having them trained by the brain.



because of not only their advantages in neuromorphic and brain-inspired chip implementation,<sup>[42a]</sup> but also their recently demonstrated capabilities to interconnect biological neurons with those neuromorphic processors.<sup>[91]</sup> This will potentially allow performance enhancement of neuromorphic and brain-inspired processors by having them trained by biology.<sup>[92]</sup> The extended discussion on this aspect is in the Bio-Artificial-Intelligence Fusion subsection below.

Certainly, memristive technologies are emerging subjects that are still under improvements. The application of memristive technologies in biotransducing and processing is an even newer area of research. While concepts have been proved indicating promising results such as the superior energy efficiency for artificial neural network implementation,<sup>[42a]</sup> and biosignal processing,<sup>[59,60]</sup> many of the memristor-based demonstrations are from prototype devices without the cointegration of dedicated CMOS peripheral circuitry.<sup>[50,58,87]</sup> This not only makes it indirect to estimate the performance of a complete memristor-based system but is also not exerting the technology's full potential. Many of the memristor-based designs are using old CMOS technologies which limits the performance of the peripheral circuitry. For example, in Table S2 (Supplementary Information), higher energy and area efficiency was achieved with a nonmemristor-based design,<sup>[92b]</sup> benefiting from the advantages of the 7 nm CMOS technology which is 8 generations newer than the CMOS technology used in a memristor-based counterpart, and the CMOS peripheral circuits were the main limiting factors for the latency, power consumption, and area occupation of the memristor-based design.<sup>[42a]</sup> Since memristor integration is only possible at wafer-level processing requiring CMOS fabrication with full mask sets, typically old CMOS technology (e.g., 130, 180 nm, etc.) was used for economic considerations.<sup>[92c]</sup> Besides, the peripheral circuits were not optimized yet for performance considering the aim of these designs are to showcase the potential of memristors with the highest priority. In the future, the codevelopment of the CMOS part, and optimization and innovation at system level will be compulsory to demonstrate the overall performance superiority when all components and practicalities required for the end application are taken into account.

## 7. Future: Bio-Artificial-Intelligence Fusion

Integrated AI, including advanced programming functions (pattern analysis and classification algorithms), can be a key link between the biological data acquisition and analysis. Such bio-AI schemes may serve in big-data processing, in self-learning/adaption systems, also holding great promise for the realization of continuous health monitoring and cloud-connected point-of-care devices for advanced diagnostics. Although the increasing progress in the field of bio-AI toward healthcare, many challenges remain and the interest goes toward the development of low-power bio-AI systems demonstrating miniaturization, scalability, and integration properties, for the creation of high-density sensors, combined with low cost, high quality (seamless, safe, nontoxic, biocompatible) biointerfacing capabilities, enabling highly sensitive body-to-signal transduction with high signal-to-noise ratio.<sup>[93]</sup>

Memristive technologies, holding an active role in transducing and processing of chemical and electrical biological data while

maintaining their properties (beyond von Neumann,<sup>[94]</sup> scalable, and low-power systems) in a wide range of materials (inorganic/organic, rigid/soft) consist excellent candidates for bio-AI systems and for pivotal building blocks for bioartificial hybrids, seamlessly linking real with artificial components.<sup>[95]</sup> Memristive/neuromorphic devices connected to the electrical outputs of neurons ultimately depict changes in their synaptic weight,<sup>[42a]</sup> while such technologies were also utilized for functionally coupling live neurons in rat brain slices in a unidirectional, activity-dependent paradigm.<sup>[52]</sup> Memristive synapses efficiently support neuronal synchronization, as demonstrated in a two-neuron network. The similarity of the spike-timing features of the memristive synapse with those natural excitatory synapses is demonstrated along with the possibility to control the magnitude of memristive coupling by the neuronal activity. Memristive elements are also employed as a bridge between brain and silicon spiking neurons, in a bidirectional way undertaking the transmission and plasticity functions of real synapses forming a hybrid network.<sup>[91]</sup> The transmission is mediated, noninvasively, by weighted stimuli through a thin film oxide microelectrode leading to responses that resemble excitatory postsynaptic potentials and the modulation of connection strength stands for the plasticity. One biological neuron and two silicon spiking neurons are connected by two memristive elements giving rise to two possible pathways: excitement of the biological part by the artificial part through the memristive element and the reverse cycle where the artificial part is stimulated by the biological one via the second memristive element. Further advancements may enable the direct cell stimulation employing memristive technologies exclusively without any additional connection and intermediating elements such as microelectrodes connected to the memristors to mediate the electronic-to-biological transmission. The realization of memristors with even lower threshold may render the devices sufficiently sensitive to respond to action potentials and transduce electrical signals directly from neurons without preamplification stages.

In perspective, even more dynamic structures and links can be achieved by the coupling of memristive/neuromorphic technologies with biological systems, supporting even more unconventional applications and enabling the development of novel diagnosis and therapy tools. Taking into consideration that the relevant first steps have already been done with application including closed-loop bidirectional BMIs,<sup>[96]</sup> lab-on-a-chip,<sup>[95a]</sup> adaptive pacemaker systems,<sup>[97]</sup> neural interfaces for the peripheral nervous system and neuromorphic interfaces with the central nervous system, neuroprostheses, artificial touch,<sup>[98]</sup> and AI-assisted and bioelectronic medicines,<sup>[99]</sup> computer schemes may be replaced by AI-embedded neuromorphic hardware where the processing unit is a collection of artificial neurons connected to the nervous system of the patient through memristive synapses in an architecture adjustable to the processing complexity. In the long-term vision, utilization of hardware accelerators undertaking the role of disease accelerators for obtaining biorealistic modeling of the diseases' progression could signify immense advancements in the diagnostics field, while ANN-based biosensing panels together with AI algorithms may serve for pattern extraction and diagnostics models out of a large throughput of biological data. Interbrain neuroprostheses applications may enable a direct link to the muscles, granting access to walking control for amputees

and hemiplegic patients with a traumatic lesion of synaptic connections between the corticospinal neurons and motor neurons in spinal cord. Restoring brain connectivity issues as in the case of traumatic injury along with other focal pathologies associated with a synaptic loss of function may be achieved by the introduction of electronic synapses reproducing the feature functions and plasticity of their biological counterparts, connecting neurons directly and replacing the damaged parts at the brain.

## Supporting Information

Supporting Information is available from the Wiley Online Library or from the author.

## Acknowledgements

The authors acknowledge the support of the EPSRC FORTE Programme (Grant No. EP/R024642/1) and the RAEng Chair in Emerging Technologies (Grant No. C1ET1819/2/93). The authors acknowledge the support of SYNCH, European Commission, FET Proactive, Grant No. 824162.

Open access funding enabled and organized by Projekt DEAL.

## Conflict of Interest

The authors declare no conflict of interest.

## Keywords

biointerfaces, biosensing, memristors

Received: October 30, 2022

Revised: January 31, 2023

Published online:

- [1] M. Mahmud, S. Vassanelli, *Front. Neurosci.* **2016**, *10*, 438.
- [2] B. Linares-Barranco, T. Serrano-Gotarredona, *Nature Precedings*, **2009**.
- [3] K. Birmingham, V. Gradinaru, P. Anikeeva, W. M. Grill, V. Píkov, B. McLaughlin, P. Pasricha, D. Weber, K. Ludwig, K. Famm, *Nat. Rev. Drug Discovery* **2014**, *13*, 399.
- [4] a) M. E. Modi, M. Sahin, *Nat. Rev. Neurol.* **2017**, *13*, 160; b) Z. Yin, G. Zhu, B. Zhao, Y. Bai, Y. Jiang, W.-J. Neumann, A. A. Kühn, J. Zhang, *Neurobiol. Dis.* **2021**, *155*, 105372.
- [5] E. R. Kandel, J. D. Koester, S. H. Mack, S. A. Siegelbaum, *Principles of Neural Science*, McGraw Hill, New York **2021**.
- [6] M. Shin, Y. Wang, J. R. Borgus, B. J. Venton, *Annu. Rev. Anal. Chem.* **2019**, *12*, 297.
- [7] A. Scimemi, M. Beato, *Mol. Neurobiol.* **2009**, *40*, 289.
- [8] K. Jackowska, P. Krysinski, *Anal. Bioanal. Chem.* **2013**, *405*, 3753.
- [9] a) M. Campbell, I. Jialal, *Physiology, Endocrine Hormones*, StatPearls Publishing, St. Petersburg, FL **2021**; b) *Nat. Immunol.* **2019**, *20*, 1557.
- [10] M. A. Zidan, J. P. Strachan, W. D. Lu, *Nat. Electron.* **2018**, *1*, 22.
- [11] S. Pi, C. Li, H. Jiang, W. Xia, H. Xin, J. J. Yang, Q. Xia, *Nat. Nanotechnol.* **2019**, *14*, 35.
- [12] A. C. Torrezan, J. P. Strachan, G. Medeiros-Ribeiro, R. S. Williams, *Nanotechnology* **2011**, *22*, 485203.
- [13] J. P. Strachan, A. C. Torrezan, G. Medeiros-Ribeiro, R. S. Williams, *Nanotechnology* **2011**, *22*, 505402.

- [14] J. Lee, W. D. Lu, *Adv. Mater.* **2018**, *30*, 1702770.
- [15] a) J. J. Yang, D. B. Strukov, D. R. Stewart, *Nat. Nanotechnol.* **2013**, *8*, 13; b) S. Stathopoulos, A. Khiat, M. Trapatseli, S. Cortese, A. Serb, I. Valov, T. Prodromakis, *Sci. Rep.* **2017**, *7*, 17532.
- [16] a) C. D. Krieger, D. J. Mountain, M. McLean, in *Proc. NeurIPS, Association for Computing Machinery, Barcelona* **2018**, pp. 1–7; b) T. Gokmen, Y. Vlasov, *Front. Neurosci.* **2016**, *10*, 333.
- [17] K. Sun, J. Chen, X. Yan, *Adv. Funct. Mater.* **2021**, *31*, 2006773.
- [18] M. Xu, X. Mai, J. Lin, W. Zhang, Y. Li, Y. He, H. Tong, X. Hou, P. Zhou, X. Miao, *Adv. Funct. Mater.* **2020**, *30*, 2003419.
- [19] Z. Xiao, J. Huang, *Adv. Electron. Mater.* **2016**, *2*, 1600100.
- [20] I. Valov, *Nat. Electron.* **2019**, *2*, 56.
- [21] Q. Zhao, Z. Xie, Y.-P. Peng, K. Wang, H. Wang, X. Li, H. Wang, J. Chen, H. Zhang, X. Yan, *Mater. Horiz.* **2020**, *7*, 1495.
- [22] H.-J. Koo, J.-H. So, M. D. Dickey, O. D. Velez, *Adv. Mater.* **2011**, *23*, 3559.
- [23] T. Fu, X. Liu, H. Gao, J. E. Ward, X. Liu, B. Yin, Z. Wang, Y. Zhuo, D. J. F. Walker, J. J. Yang, J. Chen, D. R. Lovley, J. Yao, *Nat. Commun.* **2020**, *11*, 1861.
- [24] I. Valov, M. Kozicki, *Nat. Mater.* **2017**, *16*, 1170.
- [25] Q. Xia, J. J. Yang, *Nat. Mater.* **2019**, *18*, 309.
- [26] C. He, J. Li, X. Wu, P. Chen, J. Zhao, K. Yin, M. Cheng, W. Yang, G. Xie, D. Wang, D. Liu, R. Yang, D. Shi, Z. Li, L. Sun, G. Zhang, *Adv. Mater.* **2013**, *25*, 5593.
- [27] Y. V. Pershin, M. Di Ventra, *Adv. Phys.* **2011**, *60*, 145.
- [28] G. Milano, S. Porro, I. Valov, C. Ricciardi, *Adv. Electron. Mater.* **2019**, *5*, 1800909.
- [29] J. Semple, D. G. Georgiadou, G. Wyatt-Moon, M. Yoon, A. Seithkan, E. Yengel, S. Rossbauer, F. Bottacchi, M. A. McLachlan, D. D. C. Bradley, T. D. Anthopoulos, *npj Flexible Electron.* **2018**, *2*, 18.
- [30] R. Waser, M. Aono, *Nat. Mater.* **2007**, *6*, 833.
- [31] D. Ielmini, R. Bruchhaus, R. Waser, *Phase Transitions* **2011**, *84*, 570.
- [32] M. Le Gallo, A. Sebastian, *J. Phys. D: Appl. Phys.* **2020**, *53*, 213002.
- [33] I. Valov, R. Waser, J. R. Jameson, M. N. Kozicki, *Nanotechnology* **2011**, *22*, 254003.
- [34] J. J. Yang, M. D. Pickett, X. Li, D. A. A. Ohlberg, D. R. Stewart, R. S. Williams, *Nat. Nanotechnol.* **2008**, *3*, 429.
- [35] K. Szot, W. Speier, G. Bihlmayer, R. Waser, *Nat. Mater.* **2006**, *5*, 312.
- [36] A. Wedig, M. Luebben, D.-Y. Cho, M. Moors, K. Skaja, V. Rana, T. Hasegawa, K. K. Adepal, B. Yildiz, R. Waser, I. Valov, *Nat. Nanotechnol.* **2016**, *11*, 67.
- [37] Y. Yang, P. Gao, S. Gaba, T. Chang, X. Pan, W. Lu, *Nat. Commun.* **2012**, *3*, 732.
- [38] M. Krems, Y. V. Pershin, M. Di Ventra, *Nano Lett.* **2010**, *10*, 2674.
- [39] a) W.-H. Chen, C. Dou, K.-X. Li, W.-Y. Lin, P.-Y. Li, J.-H. Huang, J.-H. Wang, W.-C. Wei, C.-X. Xue, Y.-C. Chiu, Y.-C. King, C.-J. Lin, R.-S. Liu, C.-C. Hsieh, K.-T. Tang, J. J. Yang, M.-S. Ho, M.-F. Chang, *Nat. Electron.* **2019**, *2*, 420; b) L. O. Chua, *Nat. Electron.* **2018**, *1*, 322; c) D.-H. Lim, S. Wu, R. Zhao, J.-H. Lee, H. Jeong, L. Shi, *Nat. Commun.* **2021**, *12*, 319; d) W. Zhang, B. Gao, J. Tang, P. Yao, S. Yu, M.-F. Chang, H.-J. Yoo, H. Qian, H. Wu, *Nat. Electron.* **2020**, *3*, 371.
- [40] a) M. Prezioso, F. Merrikh-Bayat, B. D. Hoskins, G. C. Adam, K. K. Likharev, D. B. Strukov, *Nature* **2015**, *521*, 61; b) M. D. Pickett, G. Medeiros-Ribeiro, R. S. Williams, *Nat. Mater.* **2013**, *12*, 114; c) Z. Wang, S. Joshi, S. E. Savel'ev, H. Jiang, R. Midya, P. Lin, M. Hu, N. Ge, J. P. Strachan, Z. Li, Q. Wu, M. Barnell, G.-L. Li, H. L. Xin, R. S. Williams, Q. Xia, J. J. Yang, *Nat. Mater.* **2017**, *16*, 101.
- [41] A. Mehonic, A. Sebastian, B. Rajendran, O. Simeone, E. Vasilaki, A. J. Kenyon, *Adv. Intell. Syst.* **2020**, *2*, 2000085.
- [42] a) P. Yao, H. Wu, B. Gao, J. Tang, Q. Zhang, W. Zhang, J. J. Yang, H. Qian, *Nature* **2020**, *577*, 641; b) A. Shafiee, A. Nag, N. Murali-manohar, R. Balasubramanian, J. P. Strachan, M. Hu, R. S. Williams, V. Srikumar, presented at 2016 ACM/IEEE 43rd Annual Int. Symp. Computer Architecture (ISCA), June **2016**; c) P. Chi, S. Li, C. Xu,

- T. Zhang, J. Zhao, Y. Liu, Y. Wang, Y. Xie, in *Proc. 43rd Int. Symp. Computer Architecture*, IEEE Press, Seoul, Republic of Korea **2016**; d) A. Ankit, I. E. Hajj, S. R. Chalamalasetti, G. Ndu, M. Foltin, R. S. Williams, P. Faraboschi, W.-m. W. Hwu, J. P. Strachan, K. Roy, D. S. Milojicic, in *Asplos '19*, IEEE, Seoul, South Korea **2019**, p. 715; e) M. Hu, C. E. Graves, C. Li, Y. Li, N. Ge, E. Montgomery, N. Davila, H. Jiang, R. S. Williams, J. J. Yang, Q. Xia, J. P. Strachan, *Adv. Mater.* **2018**, *30*, 1705914; f) A. Ankit, I. E. Hajj, S. R. Chalamalasetti, S. Agarwal, M. Marinella, M. Foltin, J. P. Strachan, D. Milojicic, W.-m. Hwu, K. Roy, *IEEE Trans. Comput.* **2020**, *69*, 1128; g) Q. Liu, T. Liu, Z. Liu, W. Wen, C. Yang, in *Proc. ACM/IEEE 57th Design Automation Conf. (Dac '20)*, IEEE, San Francisco, CA **2020**, pp. 1–6.
- [43] W. Wang, W. Song, P. Yao, Y. Li, J. Van Nostrand, Q. Qiu, D. Ielmini, J. J. Yang, *iScience* **2020**, *23*, 101809.
- [44] P. M. Sheridan, F. Cai, C. Du, W. Ma, Z. Zhang, W. D. Lu, *Nat. Nanotechnol.* **2017**, *12*, 784.
- [45] a) S. Park, M. Chu, J. Kim, J. Noh, M. Jeon, B. Hun Lee, H. Hwang, B. Lee, B.-g. Lee, *Sci. Rep.* **2015**, *5*, 10123; b) Z. Wang, S. Joshi, S. Savell'ev, W. Song, R. Midya, Y. Li, M. Rao, P. Yan, S. Asapu, Y. Zhuo, H. Jiang, P. Lin, C. Li, J. H. Yoon, N. K. Upadhyay, J. Zhang, M. Hu, J. P. Strachan, M. Barnell, Q. Wu, H. Wu, R. S. Williams, Q. Xia, J. J. Yang, *Nat. Electron.* **2018**, *1*, 137.
- [46] H. N. Khan, D. A. Hounshell, E. R. H. Fuchs, *Nat. Electron.* **2018**, *1*, 14.
- [47] a) A. Nurmikko, *Neuron* **2020**, *108*, 259; b) J. Putzeys, B. C. Raducanu, A. Carton, J. De Ceulaer, B. Karsh, J. H. Siegle, N. Van Helleputte, T. D. Harris, B. Dutta, S. Musa, C. M. Lopez, *IEEE Trans. Biomed. Circuits Syst.* **2019**, *13*, 1635.
- [48] N. A. Steinmetz, C. Aydin, A. Lebedeva, M. Okun, M. Pachitariu, M. Bauza, M. Beau, J. Bhagat, C. Böhm, M. Broux, S. Chen, J. Colonell, R. J. Gardner, B. Karsh, F. Kloosterman, D. Kostadinov, C. Mora-Lopez, J. O'Callaghan, J. Park, J. Putzeys, B. Sauerbrei, R. J. J. van Daal, A. Z. Vollen, S. Wang, M. Welkenhuysen, Z. Ye, J. T. Dudman, B. Dutta, A. W. Hantman, K. D. Harris, et al., *Science* **2021**, *372*, eabf4588.
- [49] M. Pachitariu, N. A. Steinmetz, N. S. Kadir, M. Carandini, K. D. Harris, in *Advances Neural Information Processing Systems 29 (NIPS 2016)* (Eds: D. Lee, M. Sugiyama, U. Luxburg, I. Guyon, R. Garnett), **2016**.
- [50] I. Gupta, A. Serb, A. Khat, R. Zeitler, S. Vassanelli, T. Prodromakis, *Nat. Commun.* **2016**, *7*, 12805.
- [51] a) I. Gupta, A. Serb, A. Khat, M. Trapatseli, T. Prodromakis, *Faraday Discuss.* **2019**, *213*, 511; b) I. Gupta, A. Serb, A. Khat, R. Zeitler, S. Vassanelli, T. Prodromakis, *IEEE Trans. Biomed. Circuits Syst.* **2018**, *12*, 351.
- [52] E. Juzekaeva, A. Nasretdinov, S. Battistoni, T. Berzina, S. Iannotta, R. Khazipov, V. Erokhin, M. Mukhtarov, *Adv. Mater. Technol.* **2019**, *4*, 1800350.
- [53] S. Goswami, S. Goswami, T. Venkatesan, *Appl. Phys. Rev.* **2020**, *7*, 021303.
- [54] X. Zhu, Q. Wang, W. D. Lu, *Nat. Commun.* **2020**, *11*, 2439.
- [55] a) K. Burelo, M. Sharifshazileh, N. Kranyenbühl, G. Ramantani, G. Indiveri, J. Sarnthein, *Sci. Rep.* **2021**, *11*, 6719; b) M. Sharifshazileh, K. Burelo, J. Sarnthein, G. Indiveri, *Nat. Commun.* **2021**, *12*, 3095.
- [56] E. Musk, *bioRxiv* **2019**, 703801.
- [57] N. Even-Chen, D. G. Muratore, S. D. Stavisky, L. R. Hochberg, J. M. Henderson, B. Murmann, K. V. Shenoy, *Nat. Biomed. Eng.* **2020**, *4*, 984.
- [58] Z. Liu, J. Tang, B. Gao, P. Yao, X. Li, D. Liu, Y. Zhou, H. Qian, B. Hong, H. Wu, *Nat. Commun.* **2020**, *11*, 4234.
- [59] Z. Liu, J. Tang, B. Gao, X. Li, P. Yao, Y. Lin, D. Liu, B. Hong, H. Qian, H. Wu, *Sci. Adv.* **2020**, *6*, eabc4797.
- [60] C. H. Cheng, P. Y. Tsai, T. Y. Yang, W. H. Cheng, T. Y. Yen, Z. Luo, X. H. Qian, Z. X. Chen, T. H. Lin, W. H. Chen, W. M. Chen, S. F. Liang, F. Z. Shaw, C. S. Chang, Y. L. Hsin, C. Y. Lee, M. D. Ker, C. Y. Wu, *IEEE J. Solid-State Circuits* **2018**, *53*, 3314.
- [61] E. Donati, M. Payvand, N. Risi, R. Krause, G. Indiveri, *IEEE Trans. Biomed. Circuits Syst.* **2019**, *13*, 795.
- [62] A. M. Hassan, A. F. Khalaf, K. S. Sayed, H. H. Li, Y. Chen, presented at 2018 40th Annual Int. Conf. IEEE Engineering Medicine Biology Society (EMBC), July **2018**.
- [63] E. Katz, S. Minko, *Chem. Commun.* **2015**, *51*, 3493.
- [64] a) Z. Yin, H. Tian, G. Chen, L. O. Chua, *IEEE Trans. Circuits Syst. II: Express Briefs* **2015**, *62*, 402; b) K. MacVittie, E. Katz, *J. Phys. Chem. C* **2013**, *117*, 24943.
- [65] S. T. Keene, C. Lubrano, S. Kazemzadeh, A. Melianas, Y. Tuchman, G. Polino, P. Scognamiglio, L. Cinà, A. Salleo, Y. van de Burgt, F. Santoro, *Nat. Mater.* **2020**, *19*, 969.
- [66] S. Carrara, *IEEE Sens. J.* **2021**, *21*, 12370.
- [67] I. Tzouvadaki, P. Jolly, X. Lu, S. Ingebrandt, G. de Micheli, P. Estrela, S. Carrara, *Nano Lett.* **2016**, *16*, 4472.
- [68] S. Ginnaram, J. T. Qiu, S. Maikap, *ACS Omega* **2020**, *5*, 7032.
- [69] S. H. Duh, J. Thornton, P. T. Kissinger, E. T. Chen, *TechConnect Briefs* **2014**, *2*, 169.
- [70] A. Tuoheti, A. Pabois, F. Puppo, I. Crespo, I. Tzouvadaki, D. Demarchi, J.-F. Delaloye, I. Xenarios, S. Carrara, M.-A. Doucey, *Br. J. Cancer* **2020**, *3*, 341.
- [71] E. T. Chen, J. Thornton, C. J. Mulchi, *Sens. Transducers J.* **2014**, *183*, 72.
- [72] B. Ibarlucea, T. Fawzul Akbar, K. Kim, T. Rim, C.-K. Baek, A. Ascoli, R. Tetzlaff, L. Baraban, G. Cuniberti, *Nano Res.* **2018**, *11*, 1057.
- [73] I. Tzouvadaki, S. Stathopoulos, T. Abbey, L. Michalas, T. Prodromakis, *Sci. Rep.* **2020**, *10*, 15281.
- [74] A. Vallero, I. Tzouvadaki, F. Puppo, M. A. Doucey, J. F. Delaloye, G. D. Micheli, S. Carrara, *IEEE Trans. Circuits Syst. I: Regul. Pap.* **2016**, *63*, 2120.
- [75] M. J. Schöning, A. Poghossian, *Analyst* **2002**, *127*, 1137.
- [76] D. B. Strukov, G. S. Snider, D. R. Stewart, R. S. Williams, *Nature* **2008**, *453*, 80.
- [77] I. V. Andrey, V. G. Ivan, P. Z. Vladimir, T. K. Aksultan, A. S. Vadim, *Entrepreneurship Sustainability Issues* **2020**, *8*, 98.
- [78] a) T. Sarkar, K. Lieberth, A. Pavlou, T. Frank, V. Mailaender, I. McCulloch, P. W. M. Blom, F. Torricelli, P. Gkoupidenis, *Nat. Electron.* **2022**, *5*, 774; b) P. Gkoupidenis, *Nat. Electron.* **2022**, *5*, 721; c) P. C. Harikesh, C.-Y. Yang, H.-Y. Wu, S. Zhang, M. J. Donahue, A. S. Caravaca, J.-D. Huang, P. S. Olofsson, M. Berggren, D. Tu, S. Fabiano, *Nat. Mater.* **2023**, *22*, 242.
- [79] Y. van de Burgt, E. Lubberman, E. J. Fuller, S. T. Keene, G. C. Faria, S. Agarwal, M. J. Marinella, A. Alec Talin, A. Salleo, *Nat. Mater.* **2017**, *16*, 414.
- [80] J. Wang, F. Qian, S. Huang, Z. Lv, Y. Wang, X. Xing, M. Chen, S.-T. Han, Y. Zhou, *Adv. Intell. Syst.* **2021**, *3*, 2000180.
- [81] D. S. Jeong, K. M. Kim, S. Kim, B. J. Choi, C. S. Hwang, *Adv. Electron. Mater.* **2016**, *2*, 1600090.
- [82] D. Khodagholy, J. N. Gelin, T. Thesen, W. Doyle, O. Devinsky, G. G. Malliaras, G. Buzsáki, *Nat. Neurosci.* **2015**, *18*, 310.
- [83] S. P. Lacour, G. Courtine, J. Guck, *Nat. Rev. Mater.* **2016**, *1*, 16063.
- [84] S. Fratini, M. Nikolka, A. Salleo, G. Schweicher, H. Sirringhaus, *Nat. Mater.* **2020**, *19*, 491.
- [85] G. Dijk, A. L. Rutz, G. G. Malliaras, *Adv. Mater. Technol.* **2020**, *5*, 1900662.
- [86] A. Schander, H. Stemmann, A. K. Kreiter, W. Lang, *Proceedings* **2017**, *1*, 511.
- [87] R. Chen, A. Canales, P. Anikeeva, *Nat. Rev. Mater.* **2017**, *2*, 16093.
- [88] a) S. Goswami, A. J. Matula, S. P. Rath, S. Hedström, S. Saha, M. Annamalai, D. Sengupta, A. Patra, S. Ghosh, H. Jani, S. Sarkar, M. R. Motapothula, C. A. Nijhuis, J. Martin, S. Goswami, V. S. Batista, T. Venkatesan, *Nat. Mater.* **2017**, *16*, 1216; b) E. J. Fuller, S. T. Keene,

- A. Melianas, Z. Wang, S. Agarwal, Y. Li, Y. Tuchman, C. D. James, M. J. Marinella, J. J. Yang, A. Salleo, A. A. Talin, *Science* **2019**, 364, 570.
- [89] E. Chicca, G. Indiveri, *Appl. Phys. Lett.* **2020**, 116, 120501.
- [90] Y. Tuchman, T. N. Mangoma, P. Gkoupidenis, Y. van de Burgt, R. A. John, N. Mathews, S. E. Shaheen, R. Daly, G. G. Malliaras, A. Salleo, *MRS Bull.* **2020**, 45, 619.
- [91] A. Serb, A. Corna, R. George, A. Khat, F. Rocchi, M. Reato, M. Maschietto, C. Mayr, G. Indiveri, S. Vassanelli, T. Prodromakis, *Sci. Rep.* **2020**, 10, 2590.
- [92] a) D. Ham, H. Park, S. Hwang, K. Kim, *Nat. Electron.* **2021**, 4, 635; b) Q. Dong, M. E. Sinangil, B. Erbagci, D. Sun, W. S. Khwa, H. J. Liao, Y. Wang, J. Chang, presented at 2020 IEEE Int. Solid-State Circuits Conference – (ISSCC), February **2020**; c) F. Cai, J. M. Correll, S. H. Lee, Y. Lim, V. Bothra, Z. Zhang, M. P. Flynn, W. D. Lu, *Nat. Electron.* **2019**, 2, 290.
- [93] X. Jin, C. Liu, T. Xu, L. Su, X. Zhang, *Biosens. Bioelectron.* **2020**, 165, 112412.
- [94] *Nat. Nanotechnol.* **2020**, 15, 507.
- [95] a) A. Mikhaylov, A. Pimashkin, Y. Pigareva, S. Gerasimova, E. Gryaznov, S. Shchanikov, A. Zuev, M. Talanov, I. Lavrov, V. Demin, V. Erokhin, S. Lobov, I. Mukhina, V. Kazantsev, H. Wu, B. Spagnolo, *Front. Neurosci.* **2020**, 14, 358; b) A. Chiolerio, M. Chiappalone, P. Ariano, S. Bocchini, *Front. Neurosci.* **2017**, 11, 70.
- [96] F. Boi, T. Moraitis, V. De Feo, F. Diotalevi, C. Bartolozzi, G. Indiveri, A. Vato, *Front. Neurosci.* **2016**, 10, 563.
- [97] E. Donati, R. Krause, G. Indiveri, arXiv:2102.09630 **2021**.
- [98] S. Raspopovic, A. Cimolatto, A. Panarese, F. Vallone, J. Del Valle, S. Micera, X. Navarro, *J. Neurosci. Methods* **2020**, 337, 108653.
- [99] D. Berco, D. Shenp Ang, *Adv. Intell. Syst.* **2019**, 1, 1900003.
- [100] M. Giordani, M. Sensi, M. Berto, M. Di Lauro, C. A. Bortolotti, H. L. Gomes, M. Zoli, F. Zerbetto, L. Fadiga, F. Biscarini, *Adv. Funct. Mater.* **2020**, 30, 2002141.
- [101] W. Huh, D. Lee, C.-H. Lee, *Adv. Mater.* **2020**, 32, 2002092.
- [102] a) S. Pecqueur, M. M. Mastropasqua Talamo, D. Guérin, P. Blanchard, J. Roncali, D. Vuillaume, F. Alibart, *Adv. Electron. Mater.* **2018**, 4, 1800166; b) M. Cucchi, C. Gruener, L. Petrauskas, P. Steiner, H. Tseng, A. Fischer, B. Penkovsky, C. Matthus, P. Birkholz, H. Kleemann, K. Leo, *Sci. Adv.* **2021**, 7, eabh0693.
- [103] J. Selberg, M. Jafari, J. Mathews, M. Jia, P. Pansodtee, H. Dechiraju, C. Wu, S. Cordero, A. Flora, N. Yonas, S. Jannetty, M. Diberardinis, M. Teodorescu, M. Levin, M. Gomez, M. Rolandi, *Adv. Intell. Syst.* **2020**, 2, 2000140.



**Ioulia Tzouvadaki** received her Ph.D. from École Polytechnique Fédérale de Lausanne (EPFL), Switzerland. She then joined Stanford University, USA, as a postdoctoral fellow where she worked on the integration of biosensors and readout electronics for wearable in-sweat monitoring systems. She obtained an MSCA Individual Fellowship and joined the University of Southampton, UK, where she developed bio/chemical memristor sensors. She joined Ghent University in 2022 as an assistant professor at the CMST Lab (affiliated with IMEC) in the department of Electronics and Information Systems (ELIS). Her main research interests include advanced nano/micro bio-sensors and bio-sensing systems.

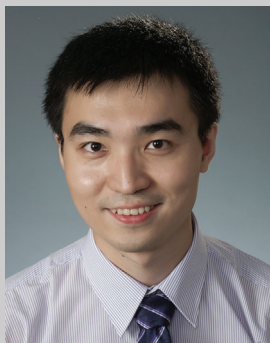


**Paschalis Gkoupidenis** earned his Ph.D. in materials science from the NCSR “Demokritos,” Athens, Greece, in 2014. During his Ph.D., his research focused on ionic transport mechanisms of organic electrolytes, for nonvolatile memories. In 2015, he started a postdoc at the Department of Bioelectronics (EMSE, France), where he focused on the development of organic neuromorphic devices based on electrochemical concepts. In 2017, he joined the Max Planck Institute for Polymer Research (Mainz, Germany), and he is currently a group leader at the Department of Molecular Electronics. The research in his group focuses on the area of organic neuromorphic electronics.





**Stefano Vassanelli** (M.D., Ph.D.) is head of the NeuroChip Laboratory and professor of physiology at the Department of Biomedical Sciences and Padua Neuroscience Center, University of Padova, Padova, Italy. He obtained his Ph.D. in molecular biology and pathology at the University of Padova and worked as postdoctoral research scientist at the Oregon Graduate Institute of Science & Technology, Portland, Oregon and at the Max-Planck Institute for Biochemistry, Department Membrane and Neurophysics, Martinsried, Germany. His research activity at the crossroad of neuroscience, materials science, and electronics focuses on neuroelectronic interfaces, brain-inspired devices, neurophysiology of brain microcircuits, and neural computation.



**Shiwei Wang** received his Ph.D. degree in microelectronics from the University of Edinburgh, UK, in 2014. He was with IMEC, Belgium from 2015 to 2020 where his research led to innovative breakthroughs in high-density neural probes and integrated brain machine interface technologies. He was an associate professor at University of Southampton from 2020 to 2022 and is now a reader in integrated-neuroelectronics at the University of Edinburgh.



**Themis Prodromakis** holds the Regius Chair of Engineering at the University of Edinburgh and is director of the Centre for Electronics Frontiers. His work focuses on developing metal-oxide resistive random-access memory technologies for embedded applications. He holds an RAEng Chair in Emerging Technologies and is adjunct professor at UTS Australia and honorary fellow at Imperial College London. He is fellow of the Royal Society of Chemistry, the British Computer Society, the IET, and the Institute of Physics.